إقـــــــرار

أنا الموقع أدناه مقدم الرسالة التي تحمل العنوان:

Characterization of Dye Sensitized Solar Cells Sensitized with the Extract of Trigonella foenum-graecum Seeds

أقر بأن ما اشتملت عليه هذه الرسالة إنما هو نتاج جهدي الخاص، باستثناء ما تمت الإشارة إليه حيثما ورد، وإن هذه الرسالة ككل أو أي جزء منها لم يقدم من قبل لنيل درجة أو لقب علمي أو بحثي لدى أي مؤسسة تعليمية أو بحثية أخرى.

DECLARATION

The work provided in this thesis, unless otherwise referenced, is the researcher's own work, and has not been submitted elsewhere for any other degree or qualification

Student's name: **Alaa Zakaria Kullab** اسم الطالب:

Signature التوقيع:

Date: التاريخ: 2015/ 10/11

Islamic University of Gaza
Deanery of Higher Studies
Faculty of Science
Department of Physics

Characterization of Dye Sensitized Solar Cells Sensitized with the Extract of Trigonella foenum-graecum Seeds

خصائص الخلايا الشمسية الصبغية باستخدام صبغة بذور الحلبة

By

Alaa Zakaria Kullab

B.Sc. in Physics, Islamic University of Gaza

Supervisors

Dr. Sofyan A. Taya
Associate Professor of Physics

Dr. Taher M. El-Agez
Associate Professor of Physics

Submitted to the Faculty of Science as a Partial Fulfillment of the Master Degree of Science (M. Sc.) in Physics

1436 – 2015

بسم الله الرحمن الرحيم

الجامعة الإسلامية – غزة
The Islamic University - Gaza

مكتب نائب الرئيس للبحث العلمي والدراسات العليا هاتف داخلي: 1150

الرقم Ref ..... ج س غ/35/

التاريخ Date 2015/10/12

نتيجة الحكم على أطروحة ماجستير

بناءً على موافقة شئون البحث العلمي والدراسات العليا بالجامعة الإسلامية بغزة على تشكيل لجنة الحكم على أطروحة الباحث/ علاء زكريا محي الدين كلاب لنيل درجة الماجستير في كلية العلوم قسم الفيزياء وموضوعها:

خصائص الخلايا الشمسية الصبغية باستخدام صبغة بذور الحلبة

Characterization of Dye-sensitized Solar Cells sensitized with the extract of Trigonella foenum-graecum seeds

وبعد المناقشة التي تمت اليوم الأحد 27 ذو الحجة 1436هـ، الموافق 2015/10/11 الساعة الحادية عشرة صباحاً، اجتمعت لجنة الحكم على الأطروحة والمكونة من:

د. سفيان عبد الرحمن تايه	مشرفاً و رئيساً	.....
د. طاهر محمد العاجز	مشرفاً	Taher M. E. Ajez
د. حسين عبد الكريم داوود	مناقشاً داخلياً	.....
د. أحمد أسعد التيان	مناقشاً خارجياً	.....

وبعد المداولة أوصت اللجنة بمنح الباحث درجة الماجستير في كلية العلوم/ قسم الفيزياء.

واللجنة إذ تمنحه هذه الدرجة فإنها توصيه بتقوى الله ولزوم طاعته وأن يسخر علمه في خدمة دينه ووطنه.

والله ولي التوفيق،،،

نائب الرئيس لشئون البحث العلمي والدراسات العليا

أ.د. عبدالرؤوف علي المناعمة

P.O. Box 108, Rimal, Gaza, Palestine fax: +970 (8) 286 0800 فاكس Tel: +970 (8) 286 0700 هاتف ص.ب. 108 الرمال، غزة، فلسطين
public@iugaza.edu.ps www.iugaza.edu.ps

Dedication

This thesis is dedicated to:

The sake of Allah, my Creator and my Master,

My great teacher and messenger, Mohammed (May Allah bless and grant him),who taught us the purpose of life,

My homeland Palestine,

The great martyrs and prisoners,

The Islamic University,

My great parents, who never stop giving of themselves in countless ways,

My beloved brothers and sisters,

My friends who encourage and support me,

and

All the people in my life who touch my heart.

Acknowledgment

In the Name of Allah, the Most Merciful, the Most Compassionate all praise be to Allah, the Lord of the worlds, and prayers and peace be upon Mohamed his servant and messenger. First and foremost, I must acknowledge my limitless thanks to Allah, the Ever-Magnificent, the Ever-Thankful, for his help and bless. I am totally sure that this work would have never become truth, without his guidance. I owe a deep debt of gratitude to our university for giving us an opportunity to complete this work. I am grateful to some people, who worked hard with me from the beginning till the completion of the present research particularly my supervisors Dr. Sofyan Taya and Dr. Taher El-Agez. I would like to take this opportunity to say warm thanks to all my beloved friends, who have been so supportive along the way of doing my thesis. I also would like to express my wholehearted thanks to my family for their generous support they provided me throughout my entire life and particularly through the process of pursuing the master degree. Because of their unconditional love and prayers, I have the chance to complete this thesis.

Abstract

Dye sensitized solar cells (DSSCs) are considered as one of the main axis for search during the last few years due to low production cost. The purpose for this thesis was to prepare DSSCs by using Titanium dioxide (TiO_2) as a semiconducting layer, FTO as conducting substrates, and ten natural dyes extracted from plant seeds such as Trigonella foenum-graecum, Apium graveolens, Rhus, Piper nigrum, Petroselinum, Ocimumbasilicum, Ammi, Peganum, Linum, and Lepidium virginicum. The absorption spectra of the ten natural dyes and current-voltage curves of the fabricated DSSCs were carried out. The results showed that the Trigonella foenum-graecum was the best dye. The effect of acid treatment of FTO substrate and TiO_2 layer was carried out using different acids. The effects of changing pH of the extracted dye solutions and of addition of ZnO layer on TiO_2 film on the performance of DSSC were examined. The results showed an efficiency drop when FTO and TiO_2 were treated by different acids and when changing pH of the extracted dye solutions. Moreover, when ZnO layer was added the efficiency also decreased. On the other hand, the fill factor of the DSSCs sensitized with Trigonella foenum-graecum exhibited an improvement when FTO was treated by H_3PO_4 and HNO_3 and when TiO_2 was treated by HNO_3. For DSSCs sensitized with Apium graveolens, the fill factors showed an enhancement when TiO_2 was treated with HNO_3 and HCl acids and the open circuit voltage was improved when FTO was treated with H_3PO_4 and HNO_3 acids. An enhancement of the open circuit voltage and fill factor was observed when the ZnO layer was added to the TiO_2 film.

Abstract in Arabic

تعد الخلايا الشمسية الصبغية المحور الرئيس للبحث خلال السنوات القليلة الماضية نظرا لقلة تكاليف تصنيعها وانتاجها. إن أهداف هذا البحث تتمثل في تحضير خلايا شمسية صبغية بإستخدام ثاني أكسيد التيتانيوم كطبقة شبه موصلة، FTO كركائز للتوصيل، و عشر صبغيات طبيعية مستخلصة من بذور النباتات وهي الحلبة، الكرفس، السماق، الفلفل الأسود، البقدونس، الريحان، الخلة، الحرمل، الكتان، وحب الرشاد. من خلال أطياف الإمتصاص ومنحنيات التيار- الجهد للأصباغ العشرة تم إختيار صبغة الحلبة كأفضل صبغة. تم دراسة أثر المعالجة لسطح FTO وطبقة شبه الموصل TiO_2 بإستخدام أحماض مختلفة، كما تم دراسة تأثير تغيير درجة الحموضة للمحلول المستخلص، ودراسة أثر إضافة طبقة ZnO لشبة الموصل TiO_2 على أداء الخلية الشمسية. أظهرت النتائج إنخفاض في الكفاءة عند معالجة سطح FTO وطبقةTiO_2بالأحماض المختلفة وعند تغيير درجة حموضة محاليل الأصباغ المستخلصة. علاوة على ذلك، عند إضافة طبقة ZnO إنخفضت الكفاءة. في الجانب الأخر ظهر تحسن في FF للخلايا الشمسية الصبغية المحسسة باستخدام صبغة الحلبة عند معالجة سطح FTO بحمضي H_3PO_4 وHNO_3 وكذلك عند معالجة TiO_2بحمض HNO_3. الخلايا الشمسية الصبغية المحسسة باستخدام صبغة الكرفس أظهرت تحسن في FF عند معالجة TiO_2 بحمضي HNO_3 وHCl و تحسن في V_{OC}عند معالجة FTO بحمضي H_3PO_4 و HNO_3. ظهر تحسن في V_{OC} و FF عند إضافة طبقة ZnO لسطح TiO_2.

CONTENTS

List of Figures

List of Tables

List of Abbreviations

J	Jhoul
^{o}k	Kelvin
^{o}C	Celisus
AM	Air mass
DSSC	Dye sensitized solar cell
CdTe	Cadmium telluride
CIGS	Copper indium gallium diselenide
a-si	Amorphous silicon
TF-si	Thin-film silicon
QDSSC	Quantum dot sensitized solar cell
PSC	Polymer solar cell
CdS	Cadmium sulfide
CdSe	Cadmium selenide
PbS	Lead sulfide
PbSe	Lead selenide
InP	Indium phosphide
MW	Mega watt
QE	Quantum efficiency
IPCE	Incident photon to electron conversion efficiency
TCO	Transparent conducting oxide

FTO	Fluorine doped tin oxide
ITO	Indium ten oxide
TiO_2	Titanium dioxide
E_c	Conduction band energy
UV	Ultraviolet
PV	Photovoltaic
S^+	Oxidized state of the dye
I^-	Iodide
I_3^-	Tri-iodide
M	Molarity
Pt	Platinum
S	Ground energy state of the sensitizer
S^*	Excited energy state of the sensitizer
S^+	Oxidized state of the sensitizer
N719	Bis (tetrabutylammonium) cis-di (thiocyanato) bis (2,2'-Bipyridine-4-COOH, 4'-COO-) ruthenium (II)
C106	cis-bis (thiocyanato) (2,2'-bipyridyl-4,4'-dicraboxylato) {4,4'-bis [5-(hexylthio)thiophen-2-y)] 2,2'-bipyridine} ruthenium(II)
LUMO	Lowest unoccupied molecular orbital
HOMO	Highest occupied molecular orbital
e^-	Electron

R_S	Series resistance
R_{SH}	Shunt resistance
I_{sc}	Short circuit current
J_{sc}	Short circuit current density
I_m	Current at maximum power point
V_m	Voltage at maximum power point
V_{oc}	Open-circuit voltage
P_{in}	Power of incident light
P_m	Maximum power
FF	Fill factor
I-V	Current-Voltage
J-V	Current density-Voltage
P-V	Power-voltage curve
AC	Alternating current
UV-VIS	Ultraviolet-Visible
IR	Infrared
ACN	Acetonitrile
KI	Potassium iodide
H_3PO_4	Phosphoric acid
HCl	Hydrochloric acid
HNO_3	Nitric acid

$C_2H_4O_2$	Acetic acid
$ZnCl_2$	Zinc chloride
ZnO	Zinc oxide
NH_4OH	Ammonium hydroxide
(a.u.)	Arbitrary units
τ_e	Electron lifetime
k_B	Boltzmann constant
T	Room temperature
STC	Standard test conditions

CHAPTER ONE

INTRODUCTION

1.1. Energy sources

There are many sources of energy in the world, such as oil energy, solar energy, wind energy, and others. All of which are classified into non-renewable and renewable sources.

1.1.1. Non-renewable energy sources

The sources of energy that formed in the earth millions of years ago and has a specific stock which will end by consumption and can't be renewed in a short period of time is called the non-renewable energy sources. Today, the world's energy supply still depends to around 90% on non-renewable energy sources, which are largely dominated by fossil fuels. As the global energy mix is widely expected to continue relying predominantly on fossil fuels in the coming decades, the question arises to what extent and how long fossil fuels will be able to sustain the supply. The projected increase in global energy demand, as well as the economic and geopolitical implications of future short comings in the supply of oil and gas, is already creating serious concerns about the security of energy supply. Especially, the transport sector, which is still almost entirely dependent on oil worldwide and would be most vulnerable to supply shortages. Previous restrictions, in addition to environmental pollutants released during the energy production process, mainly greenhouse gas emissions such as carbon dioxide, which are believed to impose a significant impact on global warming and climate change. Thus the world is forced to search for clean and renewable sources of energy.

1.1.2. Renewable energy sources

Renewable energy can be obtained from natural resources that can be constantly replenished, such as solar, hydropower, wind and biomass etc. Renewable energy

sources have the potential to meet the rising energy demand, and are expected to play an essential role in moving the world to a more secure, reliable and sustainable energy systems.

1.2. The Sun as an energy source

The only source of energy on Earth for very long time is the Sun. Recent data suggests that the Sun will continue to support life on Earth for another 1 billion years. At that point the sun will become extremely hot so that the presence of liquid water on the surface of the Earth will be impossible [1]. Meanwhile, the sun continues to output an overwhelming amount of energy. Every year 3×10^{24}J of energy hit the surface of the Earth, exceeding 10,000 times our current demand for energy [2]. Covering 0.1 % of the Earth's surface with solar cells with an efficiency of 10 % would meet our current energy demands.

1.2.1. Solar radiation

The energy from the sun has a characteristic spectrum, since the sun emits as a black body, with a temperature around 6000^{o}K. While travelling through vacuum from the sun to the earth, the shape of the spectrum is significantly altered from that of a black body. This is the extraterrestrial spectrum of light, i.e. spectrum of light outside the earth's atmosphere. Once the light enters the earth's atmosphere, the intensity is attenuated by scattering from molecules, aerosols and dust particles, as well as absorption by gases in the atmosphere [3]. The level of change is highly dependent on the amount of atmosphere the light has to pass through. When the sun is directly overhead, the distance the light has to travel to reach the earth is the lowest. As the sun moves away from the zenith through the sky, light has to pass through a greater portion of the atmosphere, and the intensity of light is reduced as it reaches the earth's surface. Assuming the sun is at an angle θ from the zenith, then the distance the light has to travel through the atmosphere is the Air Mass, where the air mass is given by the relationship

$$AM = \frac{1}{cos\theta} \quad (1.1)$$

Assuming the sun is overhead, the Air Mass is defined as 1, or AM1, and increases as it moves from the overhead position. For standard measurement conditions, AM1.5 has been used as an average spectrum for terrestrial applications, which is the global (both direct and diffuse) irradiance from the sun at an angle of approximately 48.19° from the zenith. In the case of just outside the earth's atmosphere, this is defined as AM0 since the light does not pass through any "air mass". Figure 1.1 shows the scheme for the definition of the air mass. The solar constant is defined as the amount of electromagnetic radiation per unit area reaching the Earth, measured just above the atmosphere. Its value is 1353 W/m^2 and it includes all wavelengths, not just the visible light [4]. Both spectra are shown in Figure 1.2, which highlights the amount of attenuation there is as light passes through the atmosphere. The integral of the curve over the entire wavelength range gives the total power density available from the sun under these conditions. In the case of AM1.5, this is just over 1000W/m^2 and so provides a benchmark for future experiments and measurements.

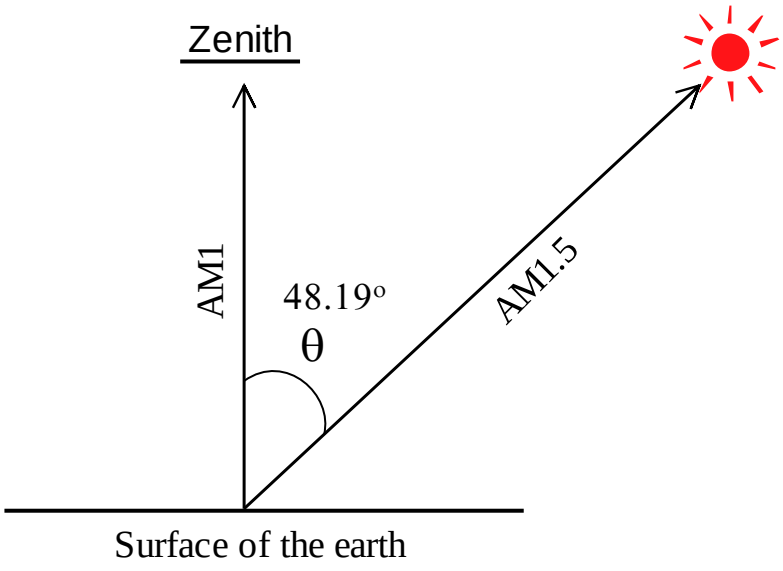

Figure 1.1. The scheme for the definition of the air mass.

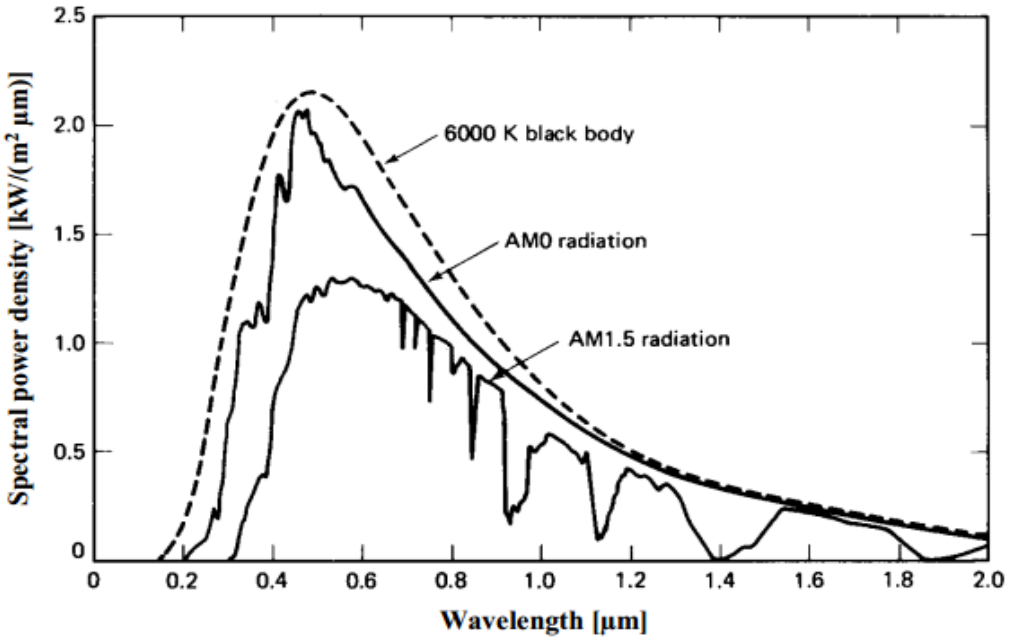

Figure 1.2. Spectral power density of sunlight. The different spectra refer to the black-body radiation at 6000K, the extraterrestrial AM0 radiation and the AM1.5 radiation [4].

1.3. Types of solar energy conversions

There are different methods by which sun radiation is converted to other forms of energy. These methods are thermal solar energy conversion, thermoelectric solar energy conversion, photoelectric solar energy conversion, and chemical solar energy conversion.

a. Thermal solar energy conversion

This method is through the use of the sun's rays directly, so that the water is heated by a device called a solar collector. This device is in abundance in the Gaza Strip, where it is mounted on rooftops. This system is not effective in winter due to the low intensity of sun radiation.

b. Thermoelectric solar energy conversion

Solar thermal technologies convert the energy of direct light into thermal energy using concentrator devices. These systems reach temperatures of several hundred

degrees with high associated energy. Electricity can then be produced using various strategies including thermal engines.

c. Photoelectric solar energy conversion

Photovoltaic directly converts photon energy into electricity. These devices use inorganic or organic semiconductor materials that absorb photons with energy greater than their band gap to promote energy carriers into their conduction band. Electron-hole pairs, or excitons for organic semiconductors, are subsequently separated and charges are collected at the electrodes for electricity generation.

d. Chemical solar energy conversion

This process is used to convert solar energy into chemical energy for energy storage in the form of chemical fuels, particularly hydrogen. Among the most significant processes for hydrogen production is direct solar water splitting in photo electrochemical cells or various thermochemical cycles such as the two-step water-splitting cycle using the Zn/ZnO redox system.

1.4. Generations of solar cells

1.4.1. First generation solar cells

The crystalline silicon solar cell was the first practical solar cell invented in 1954 by Chaplin, Fuller and Pearson. Silicon solar cell has a simple structure consisting of p-n junction. N-junction silicon is created by doping the Si with elements that contain one more valence electrons than Si does, such as Phosphorus or Arsenic. Since only four electrons are required to bond with the four adjacent silicon atoms, the fifth valence electron is available for conduction. P-junction silicon is created by doping with elements containing one less valence electrons than Si does, such as with Boron. When silicon (four valence electrons) is doped with atoms that have one less valence electrons (three valence electrons), only three electrons are available for bonding with four adjacent silicon atoms,

therefore an incomplete bond (hole) exists which can attract an electron from a nearby atom. Filling one hole creates another hole in a different Si atom. This movement of holes is available for conduction. In addition to the semiconductor junction, solar cells consist of a top and bottom metallic grid or another electrical contact that collects the separated charge carriers and connects the cell to a load. Usually, a thin layer that serves as an antireflective coating covers the topside of the cell in order to decrease the reflection of light from the cell. In order to protect the cell against the effects of outer environment during its operation, a glass sheet or other type of transparent encapsulant is attached to both sides of the cell. Silicon solar cell is still the most commercial solar cell, because it has the best efficiency among the various types of solar cells. The maximum theoretical efficiency of Si-solar cell is 33%, where the best laboratory cells can achieve up to about 25%. The commercial single-crystal Si solar cell have an efficiency in 16-20% range [5]. The major drawback of these devices is the requirement of high-grade Si. An increase in demand and an expensive manufacturing process makes these solar cells troublesome from an economic point of view.

1.4.2. Second generation solar cells

A thin-film solar cell is a second generation solar cell that is made by one or more thin film of photovoltaic material on a substrate, such as glass, plastic or metal. Film thickness varies from a few nanometers (nm) to tens of micrometers (μm). This allows thin film cells to be flexible. Thin-film solar cells exist in different types, including cadmium telluride (CdTe), copper indium gallium diselenide (CIGS), amorphous silicon (a-Si), and other thin-film silicon (TF-Si). Thin film solar cells are much less expensive than the crystalline silicon solar cells, but the efficiency is only 6–10% [5].

1.4.3. Third generation solar cells

Up to date, the photovoltaic market is still dominated by traditional solid-state p-n junction devices usually made from crystalline or amorphous silicon. Although the

cost per watt of silicon solar cells has dropped significantly over the past decade, these devices are still expensive to compete with conventional grid electricity. It is an urgent task to develop much cheaper photovoltaic devices with reasonable efficiency for widespread application of photovoltaic technology. In this context, a new type of photovoltaic devices called dye sensitized solar cells (DSSCs) based on nanocrystalline TiO_2 was developed by O'Regan and Grätzel in 1991 [6]. This type of solar cells is featured by their relatively high efficiency (exceeding 11% at full sunlight) and low fabrication cost (1/10–1/5 of silicon solar cells) [7]. Since the birth of DSSCs, great efforts have been devoted to making these devices more efficient and stable. Long-term stability tests show good prospect of DSSCs for domestic devices and decorative applications in this century. DSSCs will be presented in details in chapter two. Quantum dot sensitized solar cell (QDSSC) is considered to be a simple analogue of DSSC. The replacement of the organic dye with quantum dot (QD) sensitizers like CdS, CdSe, PbS, PbSe and InP was the only obvious difference between them. On the other hand, the basic cell mechanisms including charge separation by the sensitizer, charge transport in both the mesoporous electrode and the electrolyte, and the recombination paths seem to be similar to those of DSSC. The replacement of DSSC by QDSSC prompt by their absorption coefficient which is higher than most dyes, and the size confinement that allows tailoring of their absorption spectrum. New possibilities were opened for third generation solar cell by using QDs like multiple carrier generation and hot electron injection. Anyway, the low conversion efficiency compared to DSSC analogue in spite of great potential of it. The charge separation and recombination process at the TiO_2/QD/electrolyte junctions was the reason for low efficiencies of QDSSC.

1.4.4. Fourth generation solar cells

The fourth generation of PV technology is called Polymer Solar Cell (PSC), which combines the low cost and flexibility of polymer thin films with the stability of inorganic nanostructure in order to improve the optoelectronic properties of the

low cost thin film PVs. Polymer Solar Cell (PSC) devices are diodes that generate a photocurrent when light is incident upon their active layer. The active layer consists two sub-layers: a conjugated polymer layer (s) and a second layer of organic and/or inorganic material. The conjugated polymer (electron donor) is responsible for absorbing light and donating an electron to the organic/inorganic material (electron acceptor), which then transfers electrons to the anode. The polymer donors are typically polythiophenes or poly (pphenylene vinylene) derivatives that behave like semiconductors but are of a plastic material. The polymer molecular structures have overlapping pi-bonds allowing electrons and holes to move between energy levels upon excitation. Photoelectric manipulation of electrons and holes in these uniquely structured polymers is the basis of PSCs [8]. The electron acceptor layer is often comprised of nanoparticles or other polymers. Common organic electron acceptor materials include carbon nanotubes, Buckminster fullerenes, phthalocyanine, perylene, and their derivatives [9]. Common inorganic acceptors include TiO_2, ZnO, Si, CdSe, PbSe, and PbS [10]. PSCs that contain inorganic acceptors are also known as hybrid solar cells.

1.5. Gaza and electricity problem

For many years now, Gaza Strip has been suffering from a chronic crisis in the electricity sector. This crisis is connected with a variety of crises which its intensity varies according to the changing circumstances and contexts that affect them. There are multiple sources of electric energy that provide Gaza with electricity. The need of the Gaza Strip's electricity is currently between 350 and 450 MW which is expected to rise up to 600 MW in case of lifting the siege imposed on gaza. There are three primary sources: first, the occupation "state" electricity company, which supplies 120 MW via ten electric lines. Second, the power station in Gaza and its theoretical capacity is to produce 140 MW though its actual average of production is only 80 MW due to its dependency on the amount of fuel available for the production of electricity. Third, the Egyptian electricity grid that supplies Gaza with around 27 MW through two main electric lines. This

means that the total electricity quantity available from the three sources is about 230 MW with a seasonal variation of the electricity needs of Gaza that reach its peak to 440 MW in summer and winter. Accordingly, this shows a large deficit up to more than 150 MW, representing 35 % to 40% of the total needs of electricity, which is largely influenced by the change in the supply and demand causing a power failure. In recent times, there has been a remarkable complexity in the electricity crisis due to problematic issues in the three previously-mentioned sources of production. Power production of the Palestinian power station has fallen because of lack of fuel to run the station, as most of the fuel was brought from Egypt through tunnels that were destroyed, In addition, there are security and technical difficulties that hinder the entry of the Qatari fuel to enter Gaza to run the station. On another aspect, the occupation side refuses sometimes to provide Gaza with electricity in light of not paying the electricity bill to the occupation "state" company which is, in part, a result of the poor collection of electricity prices from its customers.

1.6. The photovoltaic effect

Photovoltaic devices operate on the principle that photons falling on a material can excite electrons. However, these electrons will only remain at this higher energy state for a very short period of time before returning to their original energy level. To collect these electrons, and allow for generation of electric current, semiconductors are used to allow current to travel in only one direction. Traditionally, solar cells are made from p and n-type doped silicon. The n-type has free extra electrons and the p-type has extra holes. When these two materials are placed in contact with each other, a p-n junction is created. Some of the electrons from the n-type will flow into the p-type to fill the holes. This will lead to charge separation across the junction, and the resulting electric field will eventually stop the electrons from flowing. Right in the middle of the junction there will be no mobile charge carriers left, and this is called the depletion region. As photons fall on the semiconductor, they can excite electrons to the conduction band. When an

electron is excited a hole is also created, commonly known as an electron-hole pair. If an external load exists, the electron will flow from the n-type across the external circuit and lose potential. Eventually it will end up at the p-side of the junction, filling up a hole it left behind. If the excited electron does not reach the p-n junction, recombination occurs and the electron returns to its original state eliminating the hole created before. The electron-hole pairs that recombine do not produce any external electricity. The ratio between the number of collected electron-hole pairs and the number of incident photons is known as quantum efficiency (QE), and is often measured as a function of wavelength. The QE is also known as Incident-Photon-to-Electron Conversion Efficiency (IPCE) [11].

1.6.1. Band gap

A photon's energy E is inversely proportional to its wavelength λ according to:

$$E = h\nu = \frac{hc}{\lambda} \tag{1.2}$$

where *h* is Planck's constant and c the speed of light [12].

If the energy exceeds the band gap of the semiconductor, the photon can be absorbed and an electron will be excited from the valence band to the conduction band. Electrons in the conduction band can move, which allows for electric current. The difference between the photon energy and the band gap will end up as heat. However, it has been documented that a high energy photon can give rise to multiple electron-hole pairs in certain materials, and this could possibly be used to reduced heat loss in solar cells.

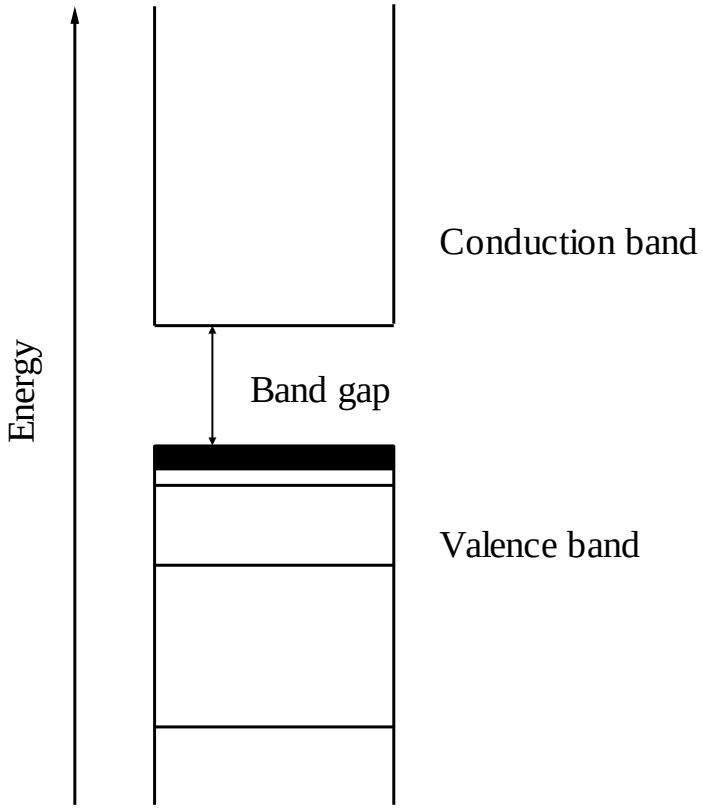

Figure 1.3. The band gap for the semiconductor.

1.7. Solar cell terminologies

A current source in parallel with a forward biased diode expresses the equivalent circuit of an ideal solar cell. Series and parallel resistances are added to account for various loss mechanisms. The main parameters of a solar cell are short-circuit current, open-circuit voltage, series resistance, shunt resistance, fill factor, and efficiency. The current–voltage relationship at a fixed cell temperature and solar radiation for the circuit in Figure1.4 is expressed in Eq. 1.3.

$$I = I_L - I_O[e^{\frac{V+IR_S}{a}} - 1] - \frac{V + IR_S}{R_{SH}} \tag{1.3}$$

where I_L the light current, I_o the diode reverse saturation current, R_s the series resistance, R_{SH} the shunt resistance, and a the modified ideality factor.

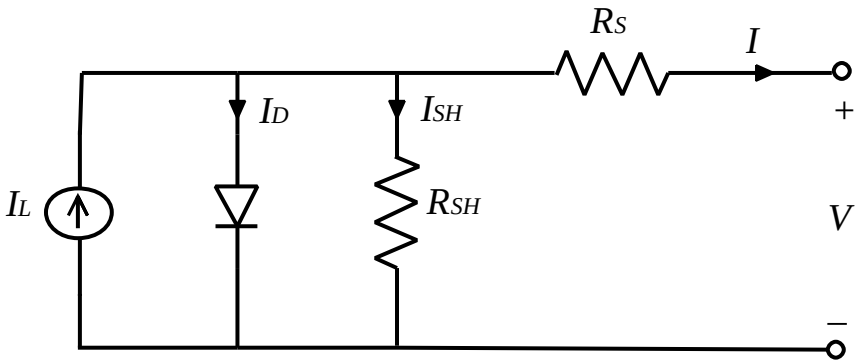

Figure 1.4. Solar cell equivalent circuit.

1.7.1. Short-circuit current

It is the current obtained from the cell when short circuited or in other words when the load resistance is zero. Solar cell current is normally represented as current density, J_{sc}

$$J_{SC} = \frac{I_{SC}}{A} \qquad (mA/cm^2) \tag{1.4}$$

where A is the effective area of the solar cell. Short circuit current is a function of the solar illumination, optical properties and charge transfer probability of the cell.

1.7.2. Open-circuit voltage

Open-circuit voltage is the maximum voltage available from a solar cell, and is obtained when a load with infinite resistance is attached to its terminals. It is a function of the semiconductor band gap and charge recombination in the cell.

1.7.3. Series resistance

Series resistance, R_s, in a solar cell is the result of contact resistance and charge transfer resistance in the semiconductor material. Series resistance reduces the fill factor (see Sec.1.7.5) affecting the maximum power output, while excessively high value of R_S can also reduce the short-circuit current. The

open-circuit voltage is not affected since, at V_{OC} the total current flow through cell itself and hence through the series resistance is zero. An approximation of the series resistance can be determined from the slope of the *IV* curve at the open-circuit voltage point.

1.7.4. Shunt resistance

Low shunt resistance provides an alternate current path for the photo-generated current causing significant power loss. The effect of low shunt resistance reduces fill factor and lowers open-circuit voltage affecting the maximum power output. The short-circuit current is not affected unless for a very low value, since at J_{SC} the total current flows through the outer path and hence through the shunt resistance. An approximation of the shunt resistance can be calculated from the slope of the *IV* curve at the short circuit current point.

1.7.5. Fill factor

The fill factor (*FF*) is a measure of the maximum power output from a solar cell. It represents the squareness of the *I-V* curve and is defined as the ratio of the maximum power to the product of V_{OC} and I_{SC} for the solar cell

$$FF = \frac{V_m \ I_m}{V_{oc} \ I_{sc}} \tag{1.5}$$

where, V_m and I_m are the voltage and current at maximum power point.

Fill factor, being a ratio of the same physical parameters, has no unit. Fill factor is a function of the series and shunt resistances of the solar cell. For DSSC, it reflects the extent of electrical and electrochemical losses during cell operation. To obtain higher fill factor, improvement of the shunt resistance and decrement of the series resistance, with reduction of the overvoltage for diffusion and charge

transfer are required. Figure 1.5 shows I_{sc}, V_{oc}, I_m, and V_m, for the typical current-voltage relationship of a solar cell.

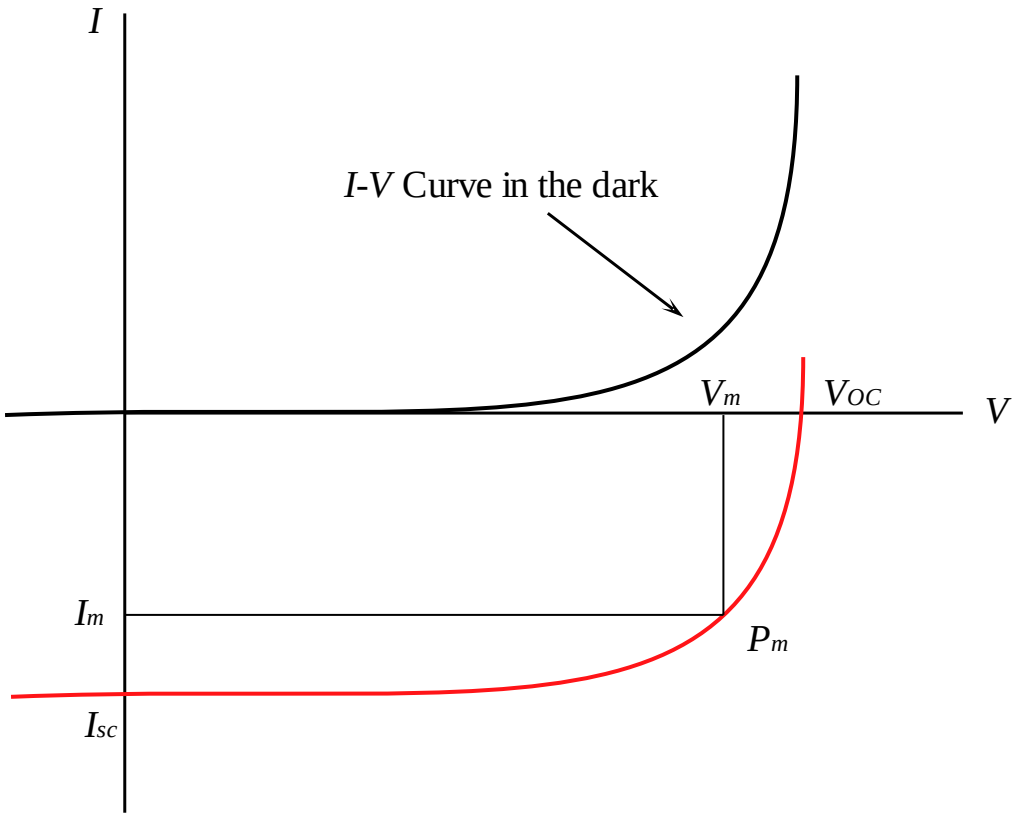

Figure 1.5. Typical current-voltage relationship of a solar cell.

1.7.6. Efficiency

The efficiency of a solar cell is defined as the ratio of maximum electrical energy output to the energy input from the sun. Thus the mathematical definition of efficiency can be written as

$$\eta_{eff} = \frac{V_{oc}\ I_{sc}\ FF}{P_{in}} = \frac{V_m\ I_m}{P_{in}} \qquad (1.6)$$

where, P_{in} is the power input from the sunlight. The cell efficiency depends on the incident light spectrum and intensity as well as operating temperature. The internationally recognized standard condition for the efficiency measurement of

solar cells is under ‘AM1.5 Global’ solar irradiation and at a temperature of 25°C [13]. Which is known as the standard test conditions (STC).

1.8. Thesis outline

The thesis was arranged into four chapters. Chapter one presents the background, general overview of photovoltaic technologies and parameters of DSSCs. Chapter two presents the components of a DSSC and its operating principle. Description of the equipments used in this work and experimental procedure are described in chapter three. All results are presented in chapter four.

CHAPTER TWO

DYE- SENSITIZED SOLAR CELLS

Introduction:

In 1991, Grätzel developed a new type of solar cells, now known as dye-sensitized solar cell (DSSC), or Grätzel cell, which represents a good alternative to the standard silicon cell. The key difference between silicon solar cells and dye sensitized solar cells described in section 1.4. A conventional DSSC consists of two conducting glass sheets as the electrodes coated with a transparent conductive layer, typically indium tin oxide. The working electrode is coated with titanium dioxide nanoparticles which have the dye adsorbed onto their surface, whereas the counter electrode, is coated with platinum or graphite. Between the two electrodes, there is an electrolyte solution that contains the redox couple that regenerates the dye. Figure 2.1 represent the diagram of conventional DSSC.

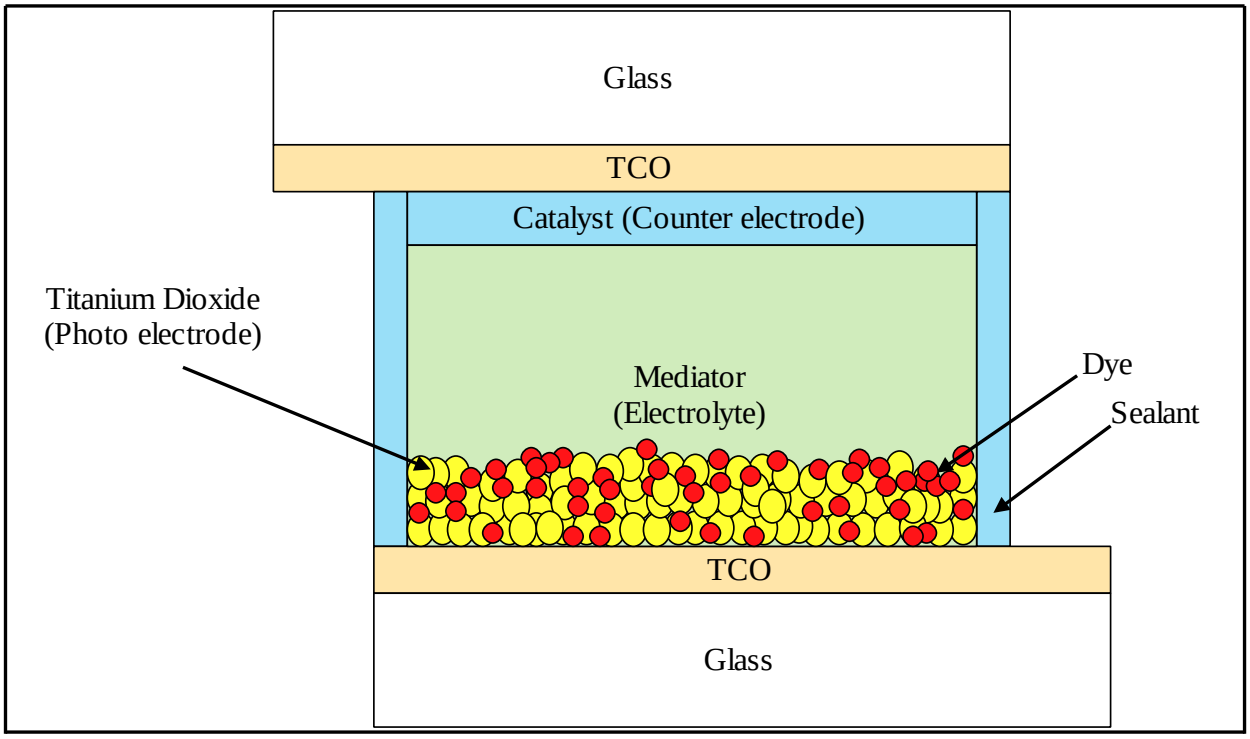

Figure 2.1. Dye-sensitized solar cell diagram.

2.1. DSSC Components:

2.1.1. Conducting substrates

The electrodes of the standard DSSC are prepared from transparent conducting oxide (TCO) between which the cell is assembled. Fluorine doped tin oxide (SnO_2 : F or FTO) and indium tin oxide (In_2O_3 : Sn or ITO) are the most frequently used as TCOs in thin film photovoltaic cells. The TCO is a degenerately doped oxide thin film deposited on a substrate which has both high transmission in the visible wavelength range allowing a high amount of photons through to the absorber, and is of high enough conductivity to collect electrons efficiently without suffering from significant ohmic losses. The TCO sandwiches the components of the DSSC together, forming a pathway for generated electrons to be removed from the device. At the working electrode, the TiO_2 network is printed onto a TCO coated glass substrate and annealed so that current collection at this interface is as an efficient process as possible. The collected electrons then travel down the TCO, travel around a circuit, and arrive at the counter electrode, which is also usually a TCO with a catalyst deposited on its surface.

2.1.2. Photo-electrodes

The photo-anode is usually composed by a nano-structured porous semiconductor on a transparent conductive oxide (TCO) glass. The choice to use a porous semiconductor is useful to increase the effective area of the anode, to permit the adsorption of a great number of sensitizer molecules. The most efficient material tested until now is titanium dioxide (TiO_2). TiO_2 is a stable, economic and versatile material. It is possible to obtain this semiconductor with different crystal phases: rutile, anatase and brookite. To realize DSSC electrodes anatase phase is used, for its large band gap, about 3.2 eV, and for the high value of the conduction band energy E_c [14]. In DSSC, the most common titanium oxide nano-structure used is composed by nanoparticles with a size from ten to a few hundred

of nanometer, even if it is possible to use other structures, such as nanowire or nanorods or different deposition techniques.

2.1.3. Sensitizing dyes

The sensitizing dye drives the electron generation in the DSSC. Without it, the wide band-gap semi-conductor would only be able to contribute electrons from high energy photons arriving from the UV, resulting in very low photo-currents. Grafting the dye to the oxide surface pushes the absorption window through into the visible, making the whole system useful for PV conversion. The dye needs to satisfy many requirements for it to be successful in a DSSC. It needs to be able to absorb a wide spectrum of light, ideally up to 900nm. It needs to easily (and permanently) attach to the oxide surface, and its excited state needs to be more negative than the conduction band of the TiO_2 to ensure fast charge injection. Conversely, the oxidized state of the dye, S^+, needs to be more positive than the redox potential, of the electrolyte so it is efficiently reduced back to its ground state. Finally, it should be chemically robust and suffer little to no change over the course of its operation.

2.1.4. The regenerative electrolyte

Whilst the working electrode provides a pathway for electrons to travel to the front, negative contact, the remaining hole must be transferred in some manner to the back, positive electrode. As is the case of classical photo-electrochemical solar cells, this transfer is mediated through an electrolyte, and in the case of the DSSC, the most successful is based on a I^-/I^-_3 redox couple in a non-aqueous solvent. To avoid confusion, the movement of holes from the sensitizer to the counter electrode is usually avoided since this may be wrongly interpreted as cation (positive) species in the electrolyte diffusing from the dye to the counter electrode. Instead, the regeneration of the oxidized dye species with an electron from the anion species in the electrolyte is more suitable. In the DSSC, the regeneration of the

oxidized sensitizer is performed by diffusion of I^- ions to the dye, which is then formed to I^-_3 which in turn is then catalytically changed back to I^- again after diffusion to the counter electrode. The electrolyte is typically made from a small concentration of iodine, around 0.05M, and a higher concentration of an iodide salt, usually around 0.6M, in a low viscosity solvent. The salt can either be a standard inorganic salt, with cations from group I elements such as lithium, sodium or potassium, or more commonly an organic cation, such as quaternary alkyl ammonium [15]. The I^-/I^-_3 redox couple has proven to be the most successful couple used in the course of DSSC research. The redox potential of the electrolyte is sufficiently high enough to ensure efficient and fast regeneration of the oxidized dye. In the DSSC, the I^- species regenerates the dye, whilst the I^-_3 species needs to be regenerated to I^-. The unwanted interception of electrons from the TiO_2 and the conducting substrate with I^-_3 contributes to the dark current of the device. A reason for the success of the I^-/I^-_3 couple is that the chemical reactions involved are relatively slow. The regeneration of the I^-_3 (forward reaction) to I^- at the counter electrode is quite fast since it is catalyzed, typically by a layer of platinum, however the back reaction from electrons in the TiO_2 to I_3^- is relatively slow since it is not catalyzed. It is the high net forward reaction which contributes to the overall success of the DSSC as a whole. The reason for the relatively slow reaction speeds involving the I^-/I^-_3 couple is that it is a two electron transfer process involving an intermediate species [16].

2.1.5. Counter-electrode catalyst

The counter electrode consists of a conducting layer on a glass substrate. For efficient regeneration of the redox couple, a layer of platinum is often coated on the substrate. In the case of the iodide/iodine redox couple, the oxidized form corresponds to triiodide and its reduction involves two electrons. The counter electrode must be catalytically active to ensure rapid reaction and low over potential. To avoid such problem, alternatives to platinum are needed. A prospective candidate is carbon. But platinum is a better catalyst for iodide/tri-

iodide couple. Because (Pt) is rare metal, therefore carbon (graphite) is used as a cheap alternative to platinum.

2.2. Operating principle

The principle of operation of DSSCs is illustrated in Fig. 2.2 which can be divided into excitation, injection, iodine reduction, and dye regeneration.

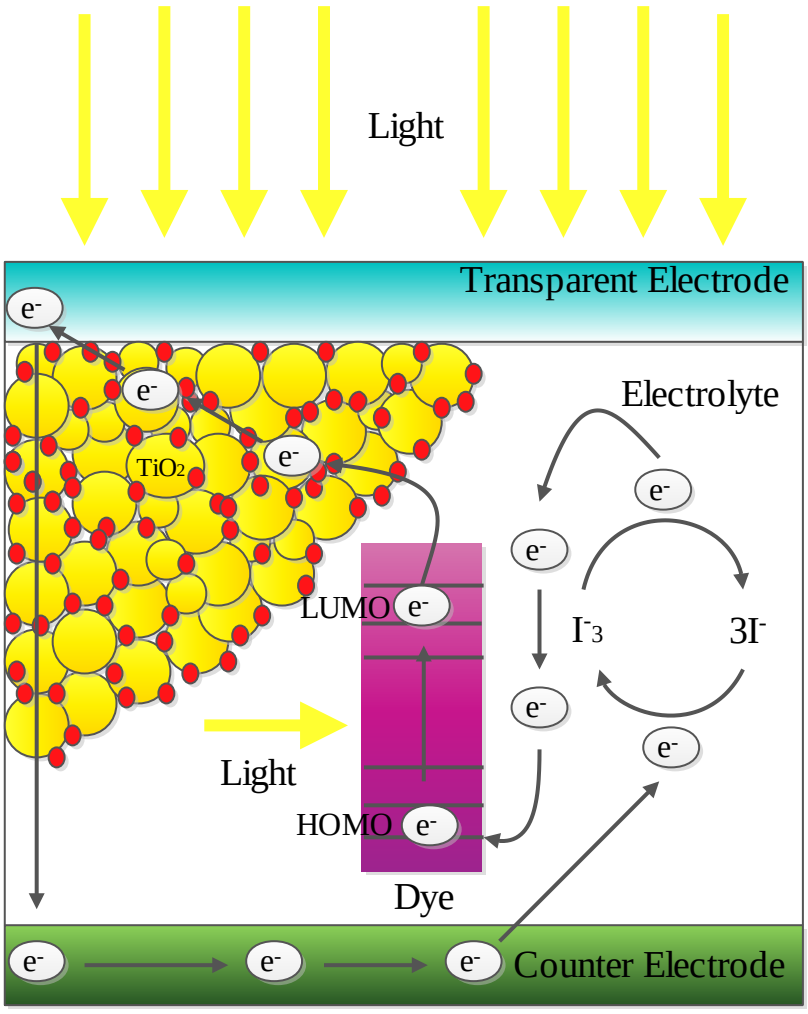

Figure 2.2. The working principle of the dye-sensitized nanostructured solar cell.

2.2.1. Excitation

The light is absorbed by a sensitizer dye molecule. The dye goes over an electronic state change from the ground (S) to the excited state (S*). For most dyes which are typically metallorganic Ru-complexes (e.g. C106 and N719), the absorption onset is in the range of 720nm corresponding to a photon energy of 1.72 eV. The lifetime of the excited state is in the order of nanoseconds [17].

$$S + h\nu \longrightarrow S^{*} \tag{2.1}$$

$$S^{*} \longrightarrow S^{+} + e^{-} \tag{2.2}$$

2.2.2. Injection

The sensitizing dye molecules are adsorbed on the surface of a wide band gap semiconductor (typically TiO_2). Upon absorption of a photon (excitation), the dye gains the ability to transfer an electron to the conduction band of the semiconductor. The internal electric field of the nanoparticles causes the electron extraction and the dye becomes oxidized (S^{+}). For efficient electron injection the lowest unoccupied molecular orbital (LUMO) of the dye has to be about 0.3 eV above the TiO_2 conduction band. The injection rate constant is in the femtosecond range for singlet state.

2.2.3. Iodine reduction

The electron travels through the outer circuit performing work, reaches the back FTO electrode, and reduces the iodine in the electrolyte. The platinum layer on the FTO acts as a catalyst for the reduction. The iodine reduction reaction is given by

$$I^{-}_{3} + 2e^{-} \longrightarrow 3I^{-} \tag{2.3}$$

The iodine reduction can also occur at the excited dye molecules causing recombination of the photo-generated electrons. For efficient charge transfer, the rate of iodine reduction at the counter electrode has to be orders of magnitude faster than the recombination at the TiO_2 - electrolyte interface.

2.2.4. Dye regeneration

The reduced iodide ion replenishes the highest occupied molecular orbital (HOMO) of the dye-regenerating its original form, and makes it ready for electron generation again. The photo anode reaction

$$2I^- \longrightarrow I_2 + 2e^- \qquad (2.4)$$

This prevents buildup of S^+, which could lead to the conduction band electrons going back to the dye molecules. The maximum output voltage equals to the difference between the Fermi level of the semiconductor and the redox potential of the mediator. Thus, the device can produce electricity from light without undergoing any permanent physical or chemical change.

2.3. State of the art

The photovoltaic technology emerged in 1839 when the physicist Alexandre Edmond Becquerel observed the generation of an electric current between two platinum electrodes immersed in an illuminated electrolyte [18]. This was the first observation of the photovoltaic effect, defined as the production of potential or electrical current between two electrodes when one of them is illuminated. Nevertheless, the photovoltaic effect remained for decades as only a scientific phenomenon without any practical application. Only in 1877, the first solar cell based on selenium was built and in 1883 Charles Fritts described this cell in detail, though the efficiency of these devices was very small, less than 1% [19]. The real photovoltaic technological developments began in 1954. Daryl Chapin, Calvin Fuller and Gerald Pearson from Bell

Telephone Laboratories, USA, developed the first silicon solar cell device using a diffused silicon p-n junction, with an efficiency of 6 %. This value of efficiency was increased to 14 % in 1960 mainly due to the work developed by Hoffman Electronics Company [20]. Many researches contributed to improve solar cells based on silicon, called the first generation solar cells. These solar cells have high production costs and moderate efficiency. The development of thin film solar cells represented the second generation solar cells and allowed to overcome some of the problems of the first generation solar cells. Second generation of solar cells offered lower costs and more efficiency. The third generation of solar cells arises to improve the efficiency of second generation thin-film technologies. Organic cells and DSSCs are representative of this new generation. The idea of dye sensitization of wide band gap semiconductors started already in the 1960s by the work of Gerischer and Tsubomura, where they used ZnO together with rose Bengal natural dye as light harvester [21]. However efficiencies remained low for many years. The breakthrough in the field came in 1991 when Michael Grätzel and Brian O'Regan demonstrated an impressive overall efficiency higher than 7% using a ruthenium based sensitizer and a porous TiO_2 layer as the semiconducting material [22]. H. EL-Ghamri prepared DSSCs by using ZnO as a semiconductor layer with eight natural dyes in 2012. The most efficient dye was Safflower which showed an efficiency of 0.1% [23]. In 2013, K. El-Refi used twenty natural dyes as photosensitizers of DSSCs and ziziphus jujuba showed the highest efficiency of 1.032% [24]. In 2015, the performance of DSSCs sensitized with purple carrot was dramatically improved using acidic pre-treatment of FTO and post-treatment of TiO_2 [25].

CHAPTER THREE

EQUIPMENTS USED IN THIS WORK AND METHODS OF FABRICATION OF DSSCs

This chapter presents a description of the instruments used in this work and the fabrication techniques of DSSCs prepared using natural dyes extracted from plant seeds. All experimental techniques including J-V characteristic curves of the fabricated cells, absorption spectra for all dyes, pre-treatment of FTO layer, post-treatment of TiO_2 layer, effect of changing pH of dye solutions, SILAR method, and open-circuit voltage decay measurement are all presented.

3.1. Description of devices

3.1.1. Autolab PGSTAT 302N

The Metrohm Autolab302N (manufactured by Autolab company) is a modular high power potentiostat/galvanostat with a maximum current of 2 A and compliance voltage of 30 V as shown in Figure 3.1. Autolab302N uses NOVA program as a control software. Setting up an experiment, measuring data and performing data analysis to produce publication ready graphs can be done in a few mouse clicks. The Autolab instruments can study the following electrochemical processes: corrosion, semiconductor electrochemistry, energy, interfacial electrochemistry, analytical and environmental electrochemistry, electrode position, nanotechnology, ultra-fast electrochemistry, and biotechnology/biosensors [26]. In this thesis Autolab302N was used for open circuit voltage decay measurements.

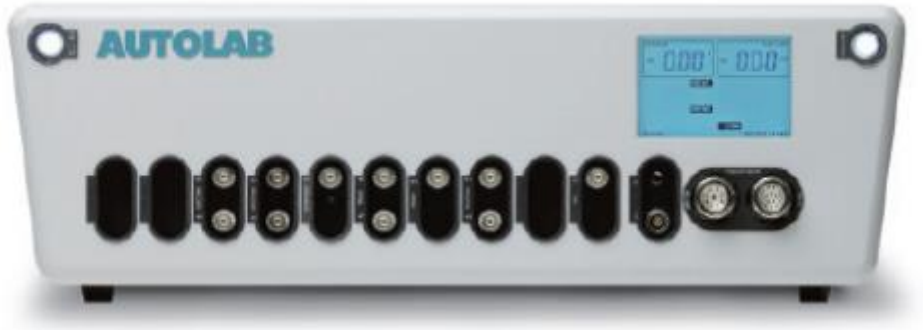

Figure 3.1. The Autolab PGSTAT 302N potentiostat/galvanostat.

3.1.2. Genesys 10S UV-VIS spectrophotometer

The Genesys 10S UV spectrophotometer (manufactured by Thermo Scientific Company) is highly flexible instruments which could be used as a standard UV/VIS spectrophotometer as well as a specialized photometer for the biotechnological laboratory as shown in Figure 3.2. GENESYS 10S UV-Vis spectrophotometer utilizes a high-intensity xenon lamp and dual-beam optical geometry to deliver unsurpassed data quality. Firing pulses of light appear only when the instrument is taking a measurement. The xenon lamp provides strong illumination from the UV to the near-IR region of the spectrum [27]. This device was used to measure the absorption spectra of dyes.

Figure 3.2. Genesys 10S UV-VIS spectrophotometer.

3.1.3. Evolution 201UV-VIS spectrophotometer

Evolution 201UV-VIS spectrophotometer (manufactured by Thermo Scientific Company) is similar to Genesys 10S UV-VIS spectrophotometer in the working principle. This device is shown in Figure 3.3 and it was used to measure the diffuse reflectance spectra of dyes adsorbed on TiO_2 films to compare between spectrophotometry before and after dying [28].

Figure 3.3. Evolution 201UV-VIS spectrophotometer.

3.1.4. Solar cell I-V measurement systems

The I-V characteristic curves under illumination were obtained using a National instruments data acquisition card (USB NI 6251) in combination with the Labview program. The I-V curves were measured at 100 mW/cm^2 illumination using a high-pressure mercury arc lamp equipped with a band-pass IR filter to avoid heating the sample. Figure 3.4 represents Solar cell simulator and I-V measurement systems.

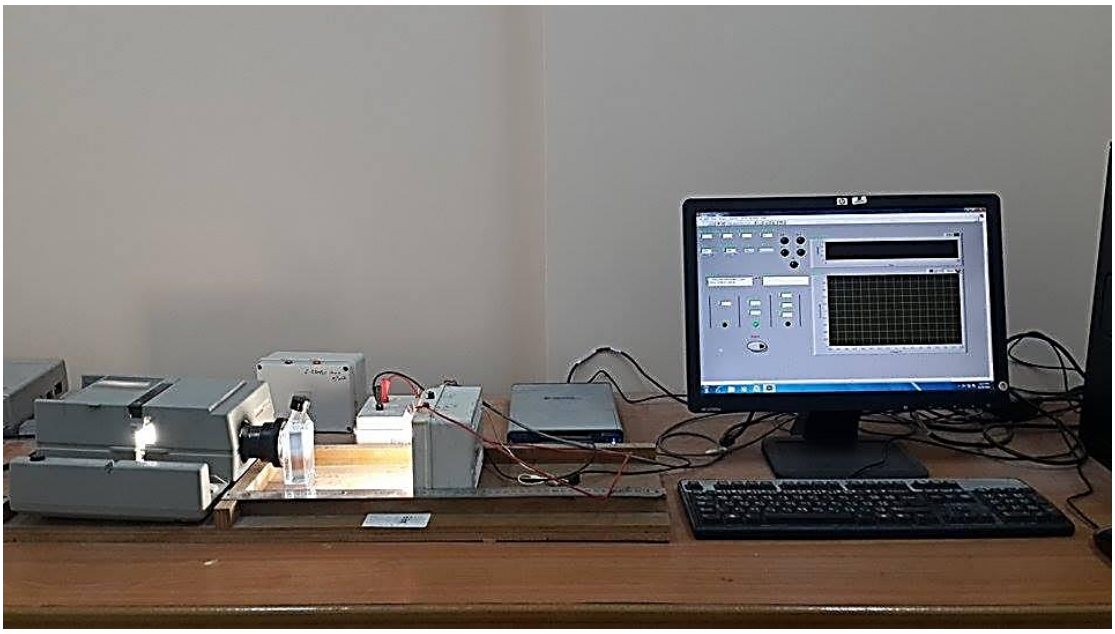

Figure 3.4. Solar cell simulator and I-V measurement systems.

3.2. Fabrication of dye-sensitized solar cells

3.2.1. Materials used in preparing solar cells

1. Fluorine-doped tin oxide (SnO_2: F) conducting glass with sheet resistance 15 Ω/cm^2, and transmission 82 -84.5% as a substrate (Xinyan Tech. Ltd, Hong Kong).

2. TiO_2 paste as a semiconducting material with particle size 10-25 nm (P25).

3. Natural dyes extracted from plants seeds as listed in Table 3.1.

4. A counter electrode fabricated from FTO-coated glass, with platinum catalyst layer.

5. A redox (I^- / I_3^-) electrolyte solution which is composed of 2ml acetonitrile (ACN), 8ml propylene carbonate (p-carbonate), 0.668gm (kI), and 0.0634gm (I_2).

6. Diluted acidic solutions: phosphoric (H_3PO_4), hydrochloric (HCl), nitric (HNO3), and acetic ($C_2H_4O_2$) acids.

7. Zinc chloride ($ZnCl_2$) and ammonium hydroxide (NH_4OH) for preparing Zinc oxide (ZnO) layer.

3.2.2. Experimental

3.2.2.1. Extraction of the natural dyes

Ten plants seeds were purchased from spice dealer. These seeds were crushed into fine powders using an electric mixer. One gram of the crushed powders were immersed in 10 ml of distilled water at room temperature and in the dark for 24 hours. After filtration of the solutions, natural dyes were obtained. The natural seeds used in this study are tabulated in Table 3.1.

Table 3.1. Natural seeds used in the extraction process.

Number of seed dye	Name of seed	Name in Arabic
SD.1	Trigonella foenum-graecum	الحلبة
SD.2	Apium graveolens	الكرفس
SD.3	Rhus	السماق
SD.4	Piper nigrum	الفلفل الأسود
SD.5	Petroselinum	البقدونس
SD.6	Ocimumbasilicum	الريحان
SD.7	Ammi	الخلة
SD.8	Peganum	الحرمل
SD.9	Linum	الكتان
SD.10	Lepidium virginicum	حب الرشاد

3.2.2.2. FTO conductive glass preparation

FTO conductive glass substrates were cut into pieces of dimensions 1.6cm×1.6cm. The glass was cleaned in a detergent solution using an ultrasonic bath for 20 min, rinsed with water and ethanol many times, and then dried using hot plate at 60 ºC for 30 min.

3.2.2.3. TiO_2 film preparation

The TiO_2 paste was prepared by adding 2 g of titanium dioxide, 4 ml distilled water, 10 µl acetyl-acetone and 50 µl Triton X-100, then the mixture was grinded for half an hour until a homogeneous paste was obtained. This procedure was proposed by K. Hara from Japan [29]. Thin TiO_2 films of dimensions 0.5cm × 0.5cm were distributed on FTO glass using doctor blade method. After spreading the paste, the films were left to dry for 5 minutes before removing the tape. The films were then heated gradually from room temperature to 450 ºC and sintered at it for 30 min using an oven and then were cooled to about 100 ºC.

3.2.2.4. Dyeing process and measurement

Thin TiO_2 films were immersed in dye solution at 100 ºC for 24 h, after that they were washed using distilled water and dried using hot plate at 70 ºC. The dyed TiO_2 electrode and platinum counter electrode were assembled to form a solar cell by sandwiching a redox (I^-/I_3^-) electrolyte solution. A solar simulator was used in the solar cell performance measurement which discussed in Sec.3.1.4.

3.2.2.5. Measuring absorption spectra of natural dyes

The absorption spectra measurements of the extracted dyes in distilled water solution were performed using a 10S UV-VIS spectrophotometer. The wavelength range of absorption spectra analysis extends from 300 to 800 nm.

3.2.2.6. Measuring absorption spectra of dye adsorbed to TiO_2

The absorption spectra of dye adsorbed to TiO_2 was performed by using Evolution 201UV-VIS spectrophotometer. Kubleka-Munk theory was used to convert diffuse reflectance spectra to absorption spectra. The resultant curve for the absorption spectra measurements of the extracted dyes in distilled water solution was compared to that adsorbed to TiO_2 to examine any shift in the absorption spectra.

Absorption spectra of dye adsorbed to TiO_2 was conducted for the best dye (Trigonella foenum-graecum).

3.2.2.7. Acidic pre-treatment of FTO surface

Three acids (phosphoric, hydrochloric, and nitric acids) were diluted with distilled water, the concentration of these acids was adjusted to 0.1M, and then FTO surface was cleaned before immersion in one of these three acids for 5 min. After that, the films were rinsed with distilled water. Then FTO surface was dried on hot plate at 70 ^{o}C for 20 min. FTO treatment was conducted for the best three dyes (Trigonella foenum-graecum, Apium graveolens, and Rhus).

3.2.2.8. Acidic post-treatment of TiO_2 film

After sintering TiO_2 films, they were immersed in one of the three acids with 0.1M concentration for 5 min. Then the same steps were followed for preparing DSSCs.

3.2.2.9. The effect of changing pH of dye solutions

This study was conducted for the best three dyes. The value of pH for each of the dye solutions was controlled using two diluted acid (hydrochloric and acetic acids). The value of the dye solution was measured without any additions. Also, the value of the dye solution was measured with addition of acids. For Trigonella foenum-graecum dye, the pH range was 3.3-6.8 and 2-6.8 with acetic and hydrochloric acids, respectively. While the pH value for Apium graveolens dye that controlled by acetic acid was in the range 3.5-6.2, when dye controlled by hydrochloric acid the pH range from 2 to 6.2. The pH range for Rhus dye controlled by acetic and hydrochloric acids was 3.5-6.5 and 2-6.5 respectively. The photovoltaic characteristics for each sample were discussed.

3.2.2.10. Using SILAR method for deposition of ZnO thin films

The successive ionic layer absorption and reaction method (SILAR) is used to create coatings on thin films for technological products such as photovoltaic cells. By allowing thin films to be coated in different chemicals at or close to room temperature, metallic films or films incorporating metallic parts can use the SILAR method and avoid possible problems with damage caused by oxidation or corrosion. Other methods of thin film deposition use the transfer of atoms to provide a coating over thin films. The SILAR method uses the transfer of ions that provides better coverage of chemicals over the film, and can result in a finer grain structure than other deposition methods. One of the advantages of the SILAR method of coating thin films is the number of different materials that can be used to create a film for a desired application. Materials that can be used in the method include temperature sensitive substrates such as polyester because the SILAR method is completed at or close to room temperature. The thin film production method known as SILAR requires the film to be immersed in the chemicals required for creating a chemical solution over the substrate. Between each immersion of the film into the chemicals, the film is rinsed using purified water to create the desired coating over the film. The main advantages of the SILAR deposition method include the ease of completing the method and the relative low cost. For small amounts of substrates to be treated using the SILAR method, the process can be completed using glass beakers. This method was conducted to improve the DSSC photovoltaic properties where it is expected to reduce the recombination of photo injected electrons without any post-treatment. Zinc chloride solutions were prepared in five different concentrations (0.005M, 0.01M, 0.05M, 0.1M, and 0.3M) by adding distilled water to zinc chloride. Drops of ammonium hydroxide were added until sludge disappears and the solution become clear. The reaction represented in equation 3.1.

$$ZnCl_2 + NH_4OH \longrightarrow ZnO + 2\,HCl + NH_3 \qquad (3.1)$$

TiO_2 films were immersed in different solutions for 15 s, then in distilled water at 90 ºC for 30 s -until TiO_2 films fully covered-. Finally, the steps for preparing dye sensitized solar cells were completed.

3.2.2.11. Open-circuit voltage decay measurements

Open-circuit voltage decay is a well-known method for studying electron recombination processes in DSSCs. In order to conduct the open-circuit voltage decay measurement, the DSSC was illuminated and a steady-state voltage was obtained. This indicated that equilibrium between electron injection and electron recombination is attained at the FTO surface. A potentiostat then monitors the decay of photovoltage, (V_{oc}), with time after interrupting the illumination.

CHAPTER FOUR

RESULTS AND DISCUSSIONS

In this chapter, experimental studies are discussed in details, including current-voltage, power-voltage curves, absorption spectra of the dyes, pre-treatment of FTO glass substrates using several acids, post-treatment of TiO_2 layer, influence of pH of the dye solution on the DSSC efficiency, using zinc oxide thin film as a barrier layer, and open circuit voltage decay measurements.

4.1. Photovoltaic results of the DSSCs

Electrical measurements of the DSSCs sensitized using the extracts of ten natural dyes are presented here. For each DSSC, the measured current density (J) versus the voltage (V) is plotted. The power density is calculated and plotted versus the voltage for each DSSC. Through the study and analysis of these curves, the cell parameters can be determined. Figure 4.1 shows the J-V characteristic curves obtained for the fabricated DSSCs using the extracts of Trigonella foenum-graecum, Apium graveolens, Rhus, Piper nigrum, Petroselinum, Ocimumbasilicum, Ammi, Peganum, Linum, and Lepidium virginicum. Figure 4.2 shows the calculated power versus the voltage for each DSSC. All the photovoltaic parameters of the fabricated DSSCs are listed in Table 4.1. Values of J_{sc} and V_{oc} were determined from the J-V curves by extrapolating the J-axis and V-axis intercepts, respectively. The maximum power point is determined from the P-V curves from which J_m and V_m can be obtained, where J_m and V_m are the current density and voltage at the maximum power point, respectively. The fill factor and the cell efficiency are calculated using Eq. (1.5) and Eq. (1.6), respectively. As can be seen from Table 4.1, the short circuit current density has a maximum value of 0.335 mA/cm^2 for the DSSC sensitized with the dye extracted from Trigonella foenum-graecum, and a minimum value of 0.024 mA/cm^2 for the DSSC sensitized with the dye extracted from Lepidium virginicum. The DSSCs sensitized with Trigonella foenum-graecum, Apium graveolens, and

Rhus have relatively high values of the short circuit current density. The open circuit voltage ranges between 0.180 V for DSSCs sensitized with Lepidium virginicum extract and 0.569 V for the cell dyed with Trigonella foenum-graecum. The DSSCs sensitized with Apium graveolens, Rhus, and Trigonella foenum-graecum have relatively high values of the open circuit voltage. The DSSCs sensitized with Rhus, Apium graveolens, and Trigonella foenum-graecum have relatively high values of the output power and efficiency. The best three dyes from ten natural dyes are Trigonella foenum-graecum, Apium graveolens, and Rhus so they will be used in the next studies. Trigonella foenum-graecum is found to be the best natural dye among other dyes with J_{sc} of 0.335 mA/cm^2, V_{oc} of 0.569 V, P_{max}= 0.098 mW, FF= 0.518 and η_{eff}= 0.098% . Figure 4.3 shows the structure of Trigonella foenum-graecum dye, from which it can be noted that it contains large number from hydroxyl group that provides it with the characteristic of formation the strong hydrogen bond between molecules of other substances. Generally, the response of the fabricated DSSCs was found to be relatively low compared to the work conducted by (a) I. Jinchu, C.O. Sreekala, and K.S. Sreelatha [30], (b) R.S. Shelke, S.B. Thombre and S.R. Patrikar [31], (c) S. Al-Bat'hi, A. Iraj, I. Sopyan [32], and (d) K.F. Moustafa, M. Rekaby, E.T. El Shenawy and N.M. Khattab [33]. The low short circuit current is due to disagreement between the energy of the excited state of the adsorbed dye and the conduction band edge of TiO_2. Moreover, the ground state of dye molecules may be considerably shifted with respect to the redox potential of I^-/I^-_3. Fast charge recombination rate and loss resulting from various competitive processes can also be responsible for the low short circuit current density. Low fill factor suggests that there is a large series resistance or a low shunt resistance in the cell. Series resistance arises from ohmic resistance, poor connection between material interfaces and low mobility of electrolyte. Low shunt resistance indicates that the current has alternative ways of crossing the cell other than the required one [34].

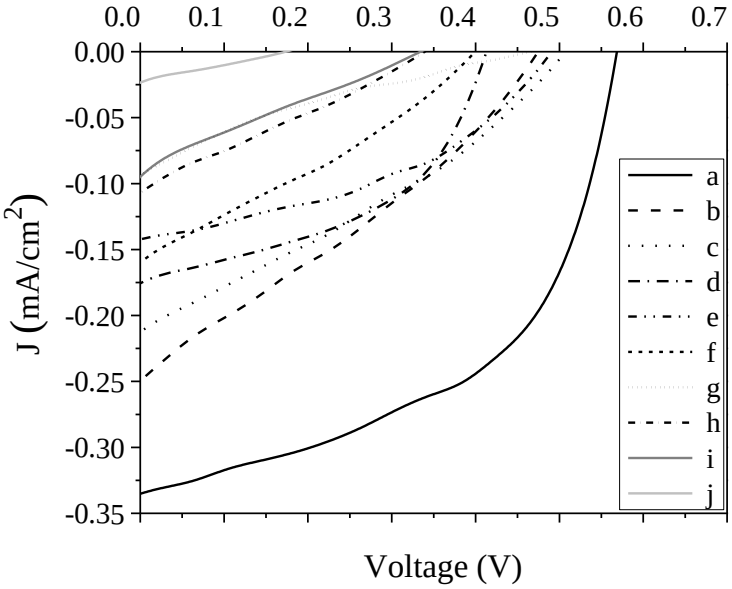

Figure 4.1. Current density-voltage characteristic curves of the DSSCs sensitized by Trigonella foenum-graecum (a), Apium graveolens (b), Rhus (c), Piper nigrum (d), Petroselinum (e), Ocimumbasilicum (f), Ammi (g), Peganum (h), Linum (i), and Lepidium virginicum (j).

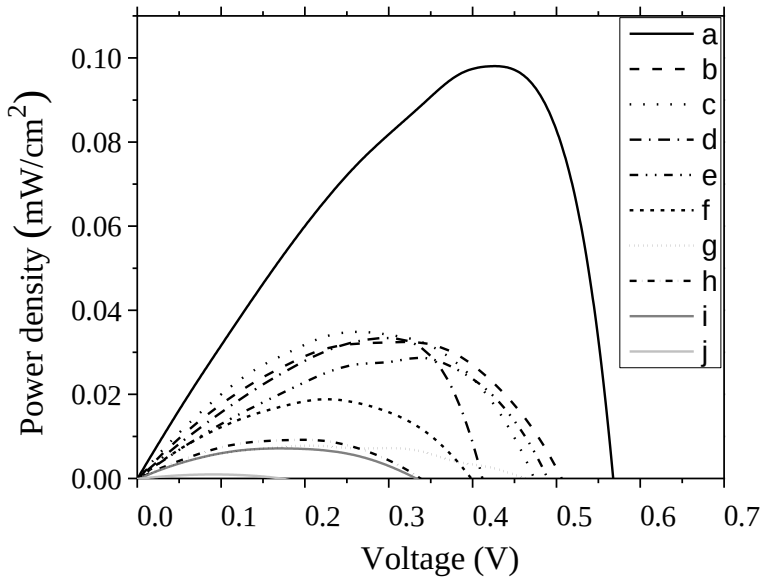

Figure 4.2. Power density-voltage characteristics curves of the DSSCs sensitized by Trigonella foenum-graecum (a), Apium graveolens (b), Rhus (c), Piper nigrum (d), Petroselinum (e), Ocimumbasilicum (f), Ammi (g), Peganum (h), Linum (i), and Lepidium virginicum (j).

Table 4.1. Photovoltaic parameters of the DSSCs sensitized by ten natural dyes.

Dye	J_{sc} (mA/cm^2)	V_{oc} (V)	J_m (mA/cm^2)	V_m (V)	P_{max} (mW)	FF	η_{eff} %
Trigonella foenum-graecum	0.335	0.569	0.234	0.422	0.098	0.518	0.098
Apium graveolens	0.251	0.474	0.093	0.341	0.032	0.267	0.032
Rhus	0.212	0.507	0.115	0.277	0.035	0.296	0.032
Piper nigrum	0.175	0.412	0.110	0.304	0.033	0.464	0.010
Petroselinum	0.142	0.490	0.082	0.342	0.029	0.138	0.010
Ocimumb-asilicum	0.159	0.400	0.082	0.232	0.019	0.299	0.004
Ammi	0.093	0.464	0.025	0.298	0.007	0.173	0.007
Peganum	0.108	0.345	0.048	0.195	0.009	0.251	0.009
Linum	0.095	0.350	0.031	0.214	0.007	0.200	0.007
Lepidium virginicum	0.024	0.180	0.001	0.099	0.001	0.023	0.0001

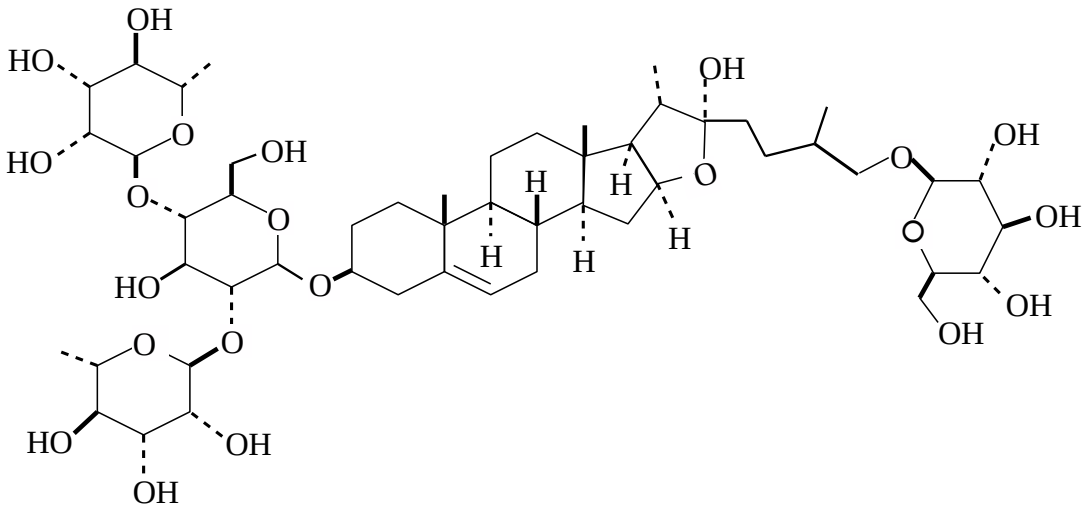

Figure 4.3. Molecular structure of Trigonella foenum-graecum extract [35].

4.2. Spectrophotometric analysis of the dye extracts

Figure 4.4 shows the UV–VIS absorption spectra of the natural dyes extracted from the seeds of Trigonella foenum-graecum, Apium graveolens, Rhus, Piper nigrum, Petroselinum, Ocimumbasilicum, Ammi, Peganum, Linum, and Lepidium virginicum in distilled water as a solvent. From Figure 4.4 (a), it can be seen that there are absorption peaks at about 311.2 nm, 327.5 nm, and 349 nm for the extract of Trigonella foenum-graecum. As can be seen from Figure 4.4 (f), there is an absorption peak at about 314.2 nm for the extract of Ocimumbasilicum. As can be seen from Figure 4.4 (i) there is an absorption peak at about 315.6 nm for the extract of Linum.

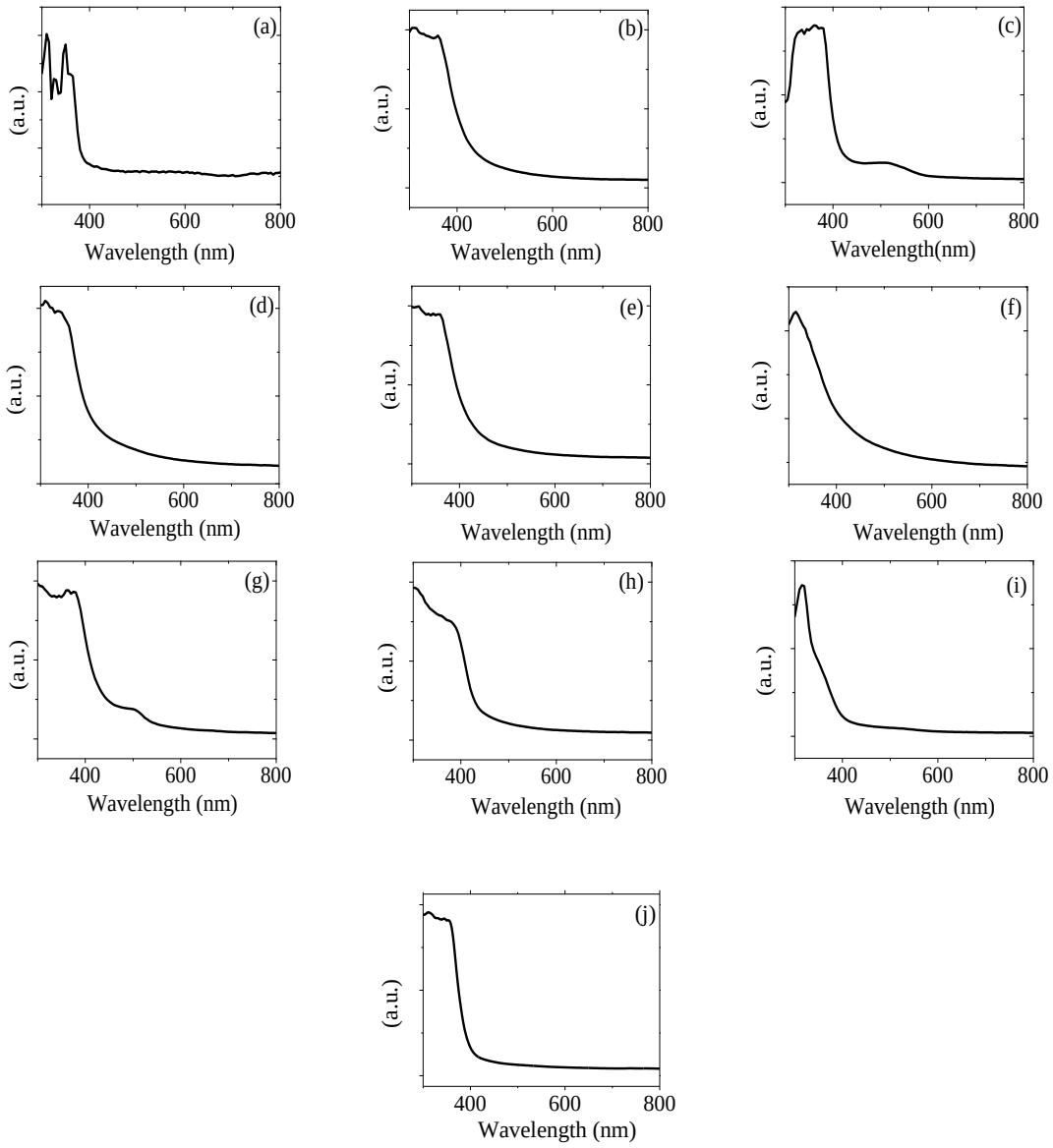

Figure 4.4. The absorption spectra of the extracts of Trigonella foenum-graecum (a), Apium graveolens (b), Rhus (c), Piper nigrum (d), Petroselinum (e), Ocimumbasilicum (f), Ammi (g), Peganum (h), Linum (i), and Lepidium virginicum (j) using distilled water as a solvent.

4.3. Measuring absorption spectra of dye adsorbed to TiO_2

Figure 4.5 shows the absorption spectra of Trigonella foenum-graecum extract in distilled water solution and Trigonella foenum-graecum dye adsorbed onto TiO_2 film. The absorption spectra for the Trigonella foenum-graecum extract in distilled water solution shows a main peak at wavelength of 349 nm. It can be observed that the absorption band of Trigonella foenum-graecum dye adsorbed onto TiO_2 film is red shifted compared to that of the Trigonella foenum-graecum extract in distilled water solution.

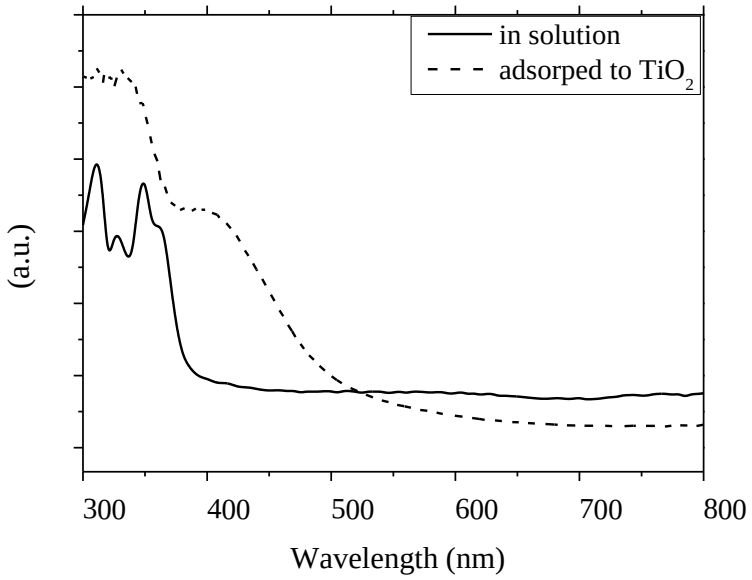

Figure 4.5. Absorption spectra of Trigonella foenum-graecum extract in distilled water solution and Trigonella foenum-graecum dye adsorbed onto TiO_2 film.

4.4. Acidic treatment of FTO

The J–V characteristics curves of the DSSCs with the pre-treatment of FTO glass substrates with 0.1M phosphoric (H_3PO_4), nitric (HNO_3), and hydrochloric (HCl) acids are shown in Figure 4.6 for Trigonella foenum-graecum, Apium graveolens, and Rhus dyes. Table 4.2 shows the photovoltaic parameters of the pre-treated DSSCs. Figure 4.6 and Table 4.2 show that the conversion efficiency of the DSSCs decreased after the pre-treatment of the FTO with any of the three acids. Treatment

of the FTO of DSSCs based on Trigonella foenum-graecum using H_3PO_4 reduced η_{eff} by 35.4%, J_{sc} by 32%, and V_{oc} by 6.3%, and improved FF by 2%. Using HNO_3 reduced η_{eff}, J_{sc}, and V_{oc} by 44.4%, 41.6%, and 9.1% respectively, but improved FF by 4.4%. When HCl was used, η_{eff} was reduced by 31%, J_{sc} by 26.5%, V_{oc} by 4%, and FF by 2.8%. From the previous discussion it can be noted that the only improvement was in FF by using HNO_3 (4.4%) and H_3PO_4 (2%) acids. For DSSCs sensitized with Apium graveolens and treated with H_3PO_4, the values of η_{eff}, J_{sc}, and FF lowered by 13.8%, 11.2%, and 9.5% respectively, while the value of V_{oc} increased by 3.9%. Treatment of FTO with HNO_3 decreased values of η_{eff} by 20%, J_{sc} by 11.2%, and FF by 15%, but the value of V_{oc} increased by 5.1%. Using HCl reduced the value of η_{eff}, J_{sc}, V_{oc}, and FF by 41.4%, 34.3%, 1.6%, and 42%, respectively. From the previous results the enhancement was only in V_{oc} when using HNO_3 and H_3PO_4 acids by 5.1% and 3.9% respectively. The pre-treatment of DSSCs based on Rhus with H_3PO_4, HNO_3, and HCl reduced J_{sc}, V_{oc}, FF, and η_{eff} as following: (a) H_3PO_4: J_{sc} by 5.7%, V_{oc} by 0.5%, FF by 13.8%, and η_{eff} by 18.2%. (b) HNO_3: J_{sc} by 25.3%, V_{oc} by 4.9%, FF by 10.7%, and η_{eff} by 36.4%. (c) HCl: J_{sc} by 23%, V_{oc} by 6.6%, FF by 27.6%, and η_{eff} by 48.5%. The results indicate that the pre-treatment by one of the three acids may lead to more recombination and less efficient carrier collection from the TiO_2 films to FTO glasses.

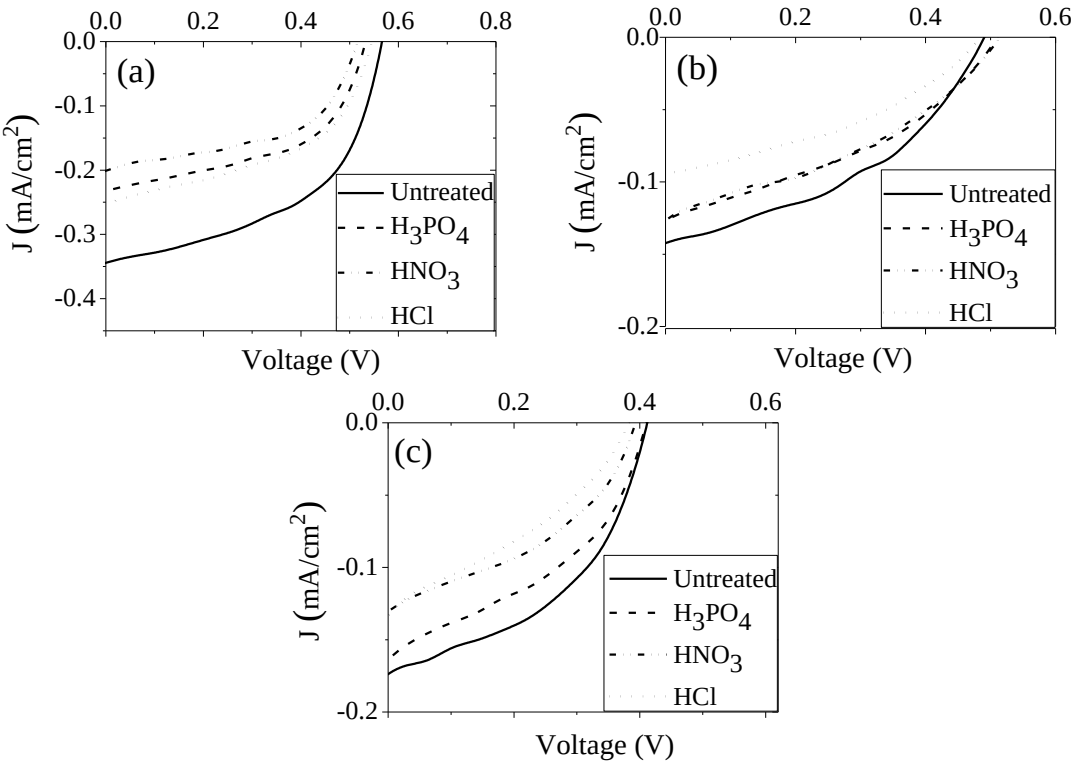

Figure 4.6. Current density versus voltage characteristic curves of DSSCs with the pre-treatment of FTO glass substrates with H_3PO_4, HNO_3, and HCl acids for Trigonella foenum-graecum dye (a), Apium graveolens dye (b), and Rhus dye (c).

Table 4.2. Photovoltaic parameters of the DSSCs with the pre-treatment of FTO glass substrates by H_3PO_4, HNO_3, and HCl acids.

Dye	FTO Pre-treatment	J_{sc} (mA/cm^2)	V_{oc} (V)	J_m (mA/cm^2)	V_m (V)	P_{max} (mW)	FF	η_{eff} %
Trigonella foenum-graecum	Untreated	0.344	0.569	0.232	0.425	0.100	0.504	0.099
	H_3PO_4	0.234	0.533	0.159	0.403	0.064	0.514	0.064
	HNO_3	0.201	0.517	0.143	0.382	0.054	0.526	0.055
	HCl	0.253	0.546	0.161	0.420	0.067	0.490	0.068
Apium graveolens	Untreated	0.143	0.490	0.086	0.342	0.029	0.420	0.029
	H_3PO_4	0.127	0.509	0.072	0.341	0.024	0.380	0.025
	HNO_3	0.127	0.515	0.069	0.338	0.023	0.357	0.023
	HCl	0.094	0.482	0.055	0.316	0.017	0.384	0.017
Rhus	Untreated	0.174	0.412	0.111	0.295	0.032	0.457	0.033
	H_3PO_4	0.164	0.410	0.089	0.298	0.027	0.394	0.027
	HNO_3	0.130	0.392	0.080	0.260	0.021	0.408	0.021
	HCl	0.134	0.385	0.068	0.251	0.017	0.331	0.017

4.5. Post-treatment of TiO_2 film surface

Figure 4.7 shows the J-V characteristics curves of the DSSCs with the post-treatment of TiO_2 electrode with phosphoric, nitric, and hydrochloric acids for Trigonella foenum-graecum, Apium graveolens, and Rhus dyes. Photovoltaic parameters of the post-treated DSSCs sensitized by Trigonella foenum-graecum, Apium graveolens, and Rhus dyes are shown in Table 4.3. As can be seen from Figure 4.7 and Table 4.3 the treated cells have lower values of efficiency in comparison with untreated cells. Low efficiency may be attributed to anchoring

reduction of the dye to the treated surface of TiO_2. Decreasing of η_{eff} by 39%, J_{sc} by 31.6%, V_{oc} by 8.4% and FF by 2.5% can be observed when TiO_2 of DSSCs based on Trigonella foenum-graecum is treated by H_3PO_4 acid. The treatment of TiO_2 using HNO_3 reduced η_{eff} by 36%, J_{sc} by 33%, and V_{oc} by 7%, but increased FF by 2.9%. The use of HCl lowered η_{eff} by 44%, J_{sc} by 36.2%, V_{oc} by 7.4%, and FF by 5.3%. Using HNO_3 in TiO_2 treatment participated in FF improvement. The post-treatment of DSSCs based on Apium graveolens dye with H_3PO_4 lowered the values of η_{eff}, J_{sc},V_{oc}, and FF by 82%, 75%, 15.8%, and 17.4%, respectively. Using HNO_3 reduced the values of η_{eff} by 25.6%, J_{sc} by 23.2%, and V_{oc} by 4.5%, and increased FF by 1.7%. The HCl acid decreased the value of η_{eff} by 35.9%, J_{sc} by 35.7%, V_{oc} by 7%, whereas the FF value was enhanced by 6%. From the previous results, using HCl and HNO_3 acids improved FF value by 6% and 1.7% respectively. For DSSCs based on Rhus and treated with H_3PO_4, there was a decrease of J_{sc} by 50.9%, V_{oc} by 5.8%, FF by 20.5%, and η_{eff} by 63.6%. Decreasing of J_{sc} by 18.9%, FF by 3.9%, and η_{eff} by 21.2% can be observed when using HNO_3 in TiO_2 treatment, but the value of V_{oc} remained fixed. The treatment by HCl reduced the values of J_{sc}, V_{oc}, FF, and η_{eff} by 33.1%, 8.2%, 30.3%, and 57.6%, respectively.

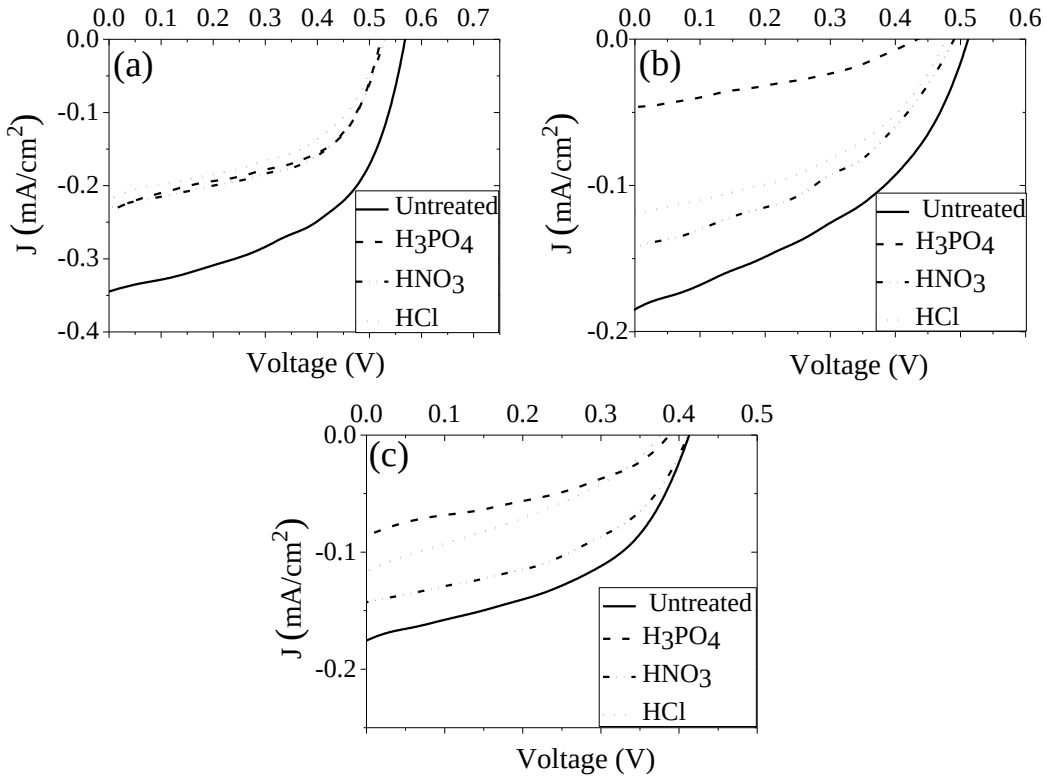

Figure 4.7. Current density versus voltage characteristic curves of DSSCs with post-treatment of TiO_2 electrode with the three acids for Trigonella foenum-graecum (a), Apium graveolens (b), and Rhus (c) dyes.

Table 4.3 Photovoltaic parameters of the DSSCs with post-treatment of TiO_2 electrode by the three acids for Trigonella foenum-graecum, Apium graveolens, and Rhus dyes.

Dye	TiO_2 Post-treatment	J_{sc} (mA/cm^2)	V_{oc} (V)	J_m (mA/cm^2)	V_m (V)	P_{max} (mW)	FF	η_{eff} %
Trigonella foenum-graecum	Untreated	0.345	0.569	0.234	0.428	0.100	0.510	0.100
	H_3PO_4	0.236	0.521	0.159	0.384	0.064	0.497	0.061
	HNO_3	0.231	0.529	0.152	0.422	0.062	0.525	0.064
	HCl	0.220	0.527	0.147	0.381	0.055	0.483	0.056
Apium graveolens	Untreated	0.185	0.513	0.112	0.351	0.039	0.414	0.039
	H_3PO_4	0.046	0.432	0.022	0.309	0.007	0.342	0.007
	HNO_3	0.142	0.490	0.086	0.341	0.029	0.421	0.029
	HCl	0.119	0.477	0.073	0.341	0.025	0.439	0.025
Rhus	Untreated	0.175	0.413	0.110	0.301	0.033	0.458	0.033
	H_3PO_4	0.086	0.389	0.047	0.259	0.012	0.364	0.012
	HNO_3	0.142	0.413	0.086	0.300	0.026	0.440	0.026
	HCl	0.117	0.379	0.057	0.248	0.014	0.319	0.014

4.6. Effect of pH of dye solution

The J-V characteristics of DSSCs sensitized with the extracts of Trigonella foenum-graecum, Apium graveolens, and Rhus at different values of pH obtained using acetic and hydrochloric acids are shown in Figure 4.8. Tables 4.4, 4.5, and 4.6 show the photovoltaic parameters of the DSSCs sensitized by Trigonella foenum-graecum, Apium graveolens, and Rhus, respectively at different pH values. Figure 4.8, and Tables 4.4, 4.5, and 4.6 shows that the conversion efficiency of the DSSCs decreased after changing the pH of all dye solutions. This

decline is probably attributable to the acid present in the dye modifies the surface state of the porous film and creates defect centers on the TiO_2 surface. These defects prevent the transfer of electrons to the TiO_2 grid from the excited state of the sensitized dye molecule, which results in lowering electron transportation efficiency and decreasing photovoltaic performance.

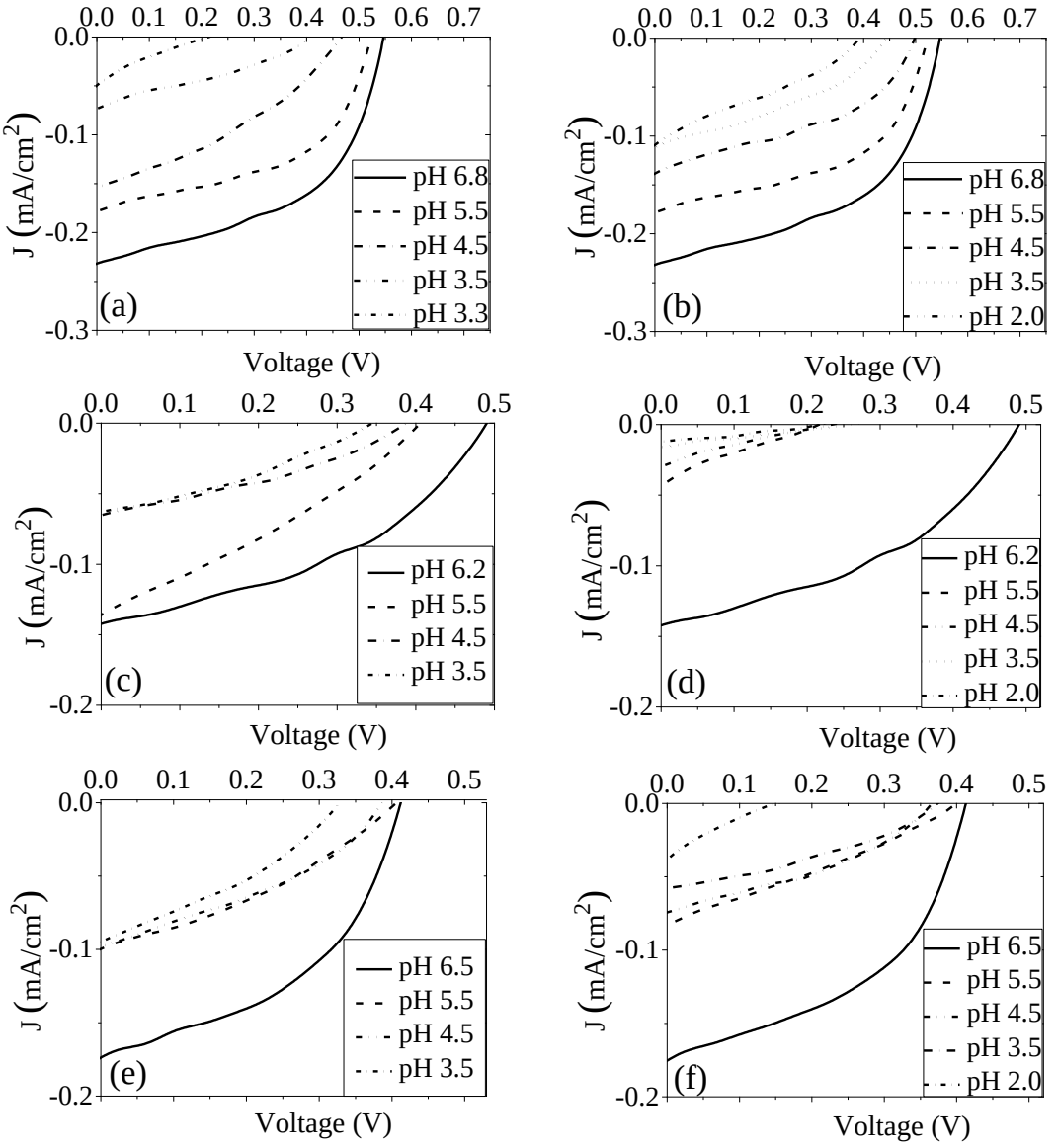

Figure 4.8. Current density versus voltage characteristic curves for DSSC sensitized with Trigonella foenum-graecum (a), Apium graveolens (c), and Rhus (e) using acetic acid to change the pH of the dye solutions and sensitized with Trigonella foenum-graecum (b), Apium graveolens (d), and Rhus (f) using hydrochloric acid to change the pH of the dye solutions.

Table 4.4. Photovoltaic parameters of the DSSCs sensitized by Trigonella foenum-graecum at different pH values using acetic acid and hydrochloric acid.

Acid type	pH	J_{sc} (mA/cm^2)	V_{oc} (V)	J_m (mA/cm^2)	V_m (V)	P_{max} (mW)	FF	η_{eff} %
Acetic acid	6.8	0.232	0.547	0.153	0.422	0.064	0.509	0.064
	5.5	0.179	0.524	0.125	0.382	0.047	0.509	0.048
	4.5	0.154	0.466	0.081	0.300	0.024	0.339	0.024
	3.5	0.075	0.405	0.042	0.221	0.009	0.306	0.009
	3.3	0.049	0.220	0.013	0.140	0.002	0.169	0.002
Hydrochloric acid	6.8	0.232	0.546	0.155	0.421	0.065	0.515	0.065
	5.5	0.179	0.523	0.124	0.383	0.041	0.507	0.047
	4.5	0.139	0.501	0.074	0.379	0.027	0.403	0.028
	3.5	0.113	0.442	0.051	0.341	0.016	0.348	0.017
	2.0	0.109	0.390	0.047	0.262	0.011	0.290	0.012

Table 4.5. Photovoltaic parameters of the DSSCs sensitized by Apium graveolens at different pH values using acetic acid and hydrochloric acid.

Acid type	pH	J_{sc} (mA/cm^2)	V_{oc} (V)	J_m (mA/cm^2)	V_m (V)	P_{max} (mW)	FF	η_{eff} %
Acetic acid	6.2	0.143	0.491	0.084	0.341	0.028	0.410	0.029
	5.5	0.136	0.410	0.071	0.235	0.016	0.299	0.017
	4.5	0.066	0.390	0.038	0.227	0.009	0.355	0.009
	3.5	0.063	0.343	0.037	0.194	0.007	0.332	0.007
Hydrochloric acid	6.2	0.142	0.490	0.085	0.340	0.029	0.415	0.029
	5.5	0.044	0.221	0.022	0.101	0.002	0.229	0.002
	4.5	0.030	0.235	0.014	0.103	0.0015	0.205	0.001
	3.5	0.017	0.259	0.006	0.169	0.001	0.230	0.001
	2.0	0.012	0.221	0.010	0.099	0.001	0.373	0.001

Table 4.6. Photovoltaic parameters of the DSSCs sensitized by Rhus at different pH values using acetic acid and hydrochloric acid.

Acid type	pH	J_{sc} (mA/cm^2)	V_{oc} (V)	J_m (mA/cm^2)	V_m (V)	P_{max} (mW)	FF	η_{eff} %
Acetic acid	6.5	0.173	0.412	0.109	0.300	0.032	0.459	0.033
	5.5	0.098	0.409	0.052	0.260	0.014	0.337	0.014
	4.5	0.098	0.387	0.054	0.261	0.014	0.372	0.014
	3.5	0.095	0.327	0.048	0.219	0.010	0.338	0.011
Hydrochloric acid	6.5	0.176	0.412	0.112	0.301	0.033	0.465	0.034
	5.5	0.083	0.400	0.042	0.223	0.009	0.282	0.009
	4.5	0.074	0.365	0.042	0.225	0.01	0.350	0.009
	3.5	0.058	0.372	0.029	0.259	0.008	0.348	0.008
	2.0	0.038	0.148	0.01	0.1	0.001	0.178	0.001

Figure 4.9 shows the DSSC efficiency as a function of the pH of the Trigonella foenum-graecum, Apium graveolens, and Rhus extract solutions using acetic acid and hydrochloric acid. As observed from the figure, the efficiency is diminished dramatically with decreasing the pH values.

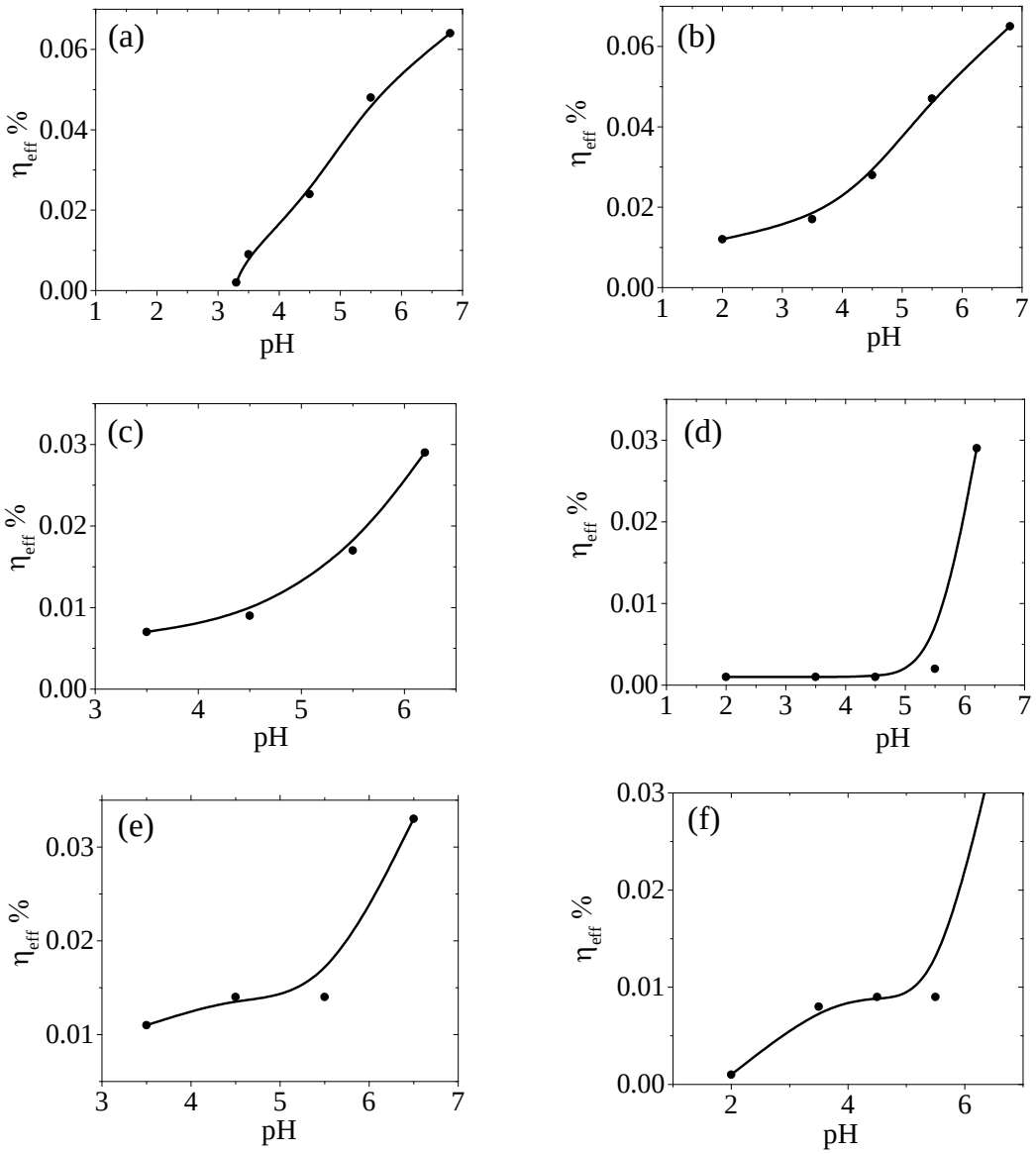

Figure 4.9. DSSC efficiency versus the pH of the extract solutions by using acetic acid: Trigonella foenum-graecum (a), Apium graveolens (c), and Rhus (e) and by using hydrochloric acid: Trigonella foenum-graecum (b), Apium graveolens (d), and Rhus (f).

4.7. Using SILAR method for deposition of ZnO thin films

The J-V characteristics of DSSCs sensitized with extracts of Trigonella foenum-graecum and treated with ZnO barrier layer deposited on TiO_2 thin film by SILAR method at different concentrations of $ZnCl_2$ solutions are shown in Figure 4.10. Table 4.7 shows the photovoltaic parameters of the DSSCs sensitized by Trigonella foenum-graecum and treated with ZnO barrier layer at different concentrations of $ZnCl_2$ solutions on TiO_2 thin film. Figure 4.11 represents the relation between molarities and different parameters for DSSCs sensitized by Trigonella foenum-graecum dye treated with ZnO layer on TiO_2 thin film. The results show that the addition of the ZnO layer increases the open-circuit voltages and fill factors and causes a sharp decrease of the photocurrent. 0.005M resulted in improving V_{oc} by 20.2% and FF by 4.1% but in reducing J_{sc} by 23.2%. 0.01M contributed to increase of V_{oc} by 15.7% and FF by 5%. However, it decreased J_{sc} by 54.3%. 0.05M enhanced V_{oc} by 11% and FF by 16.35%, while lowered J_{sc} by 67.3%. 0.1M lead to enhancement of V_{oc} by 9% and FF by 6%, and reduction of J_{sc} by 79.5%. 0.3M raised V_{oc} by 3.1% and FF by 0.56%, and diminished J_{sc} by 81.6%. The highest value of V_{oc} was at lowest concentration of treated cell with ZnO layer and when the concentration increased, the value of V_{oc} decreased. The lowest V_{oc} value was for untreated cell. It noted that 0.005M was the best concentration in increasing the open-circuit voltage value where it increased from 0.574 V to 0.690 V by 20.2%. The main reason behind the open-circuit voltage and fill factor improvements is that the addition of ZnO layer to TiO_2 thin films leads to depress the recombination process in the cells. There are several mechanisms by which the ZnO modification can cause an open-circuit voltage increase, such as the tunnel barrier effect, surface dipole effect and reducing the surface states [36].

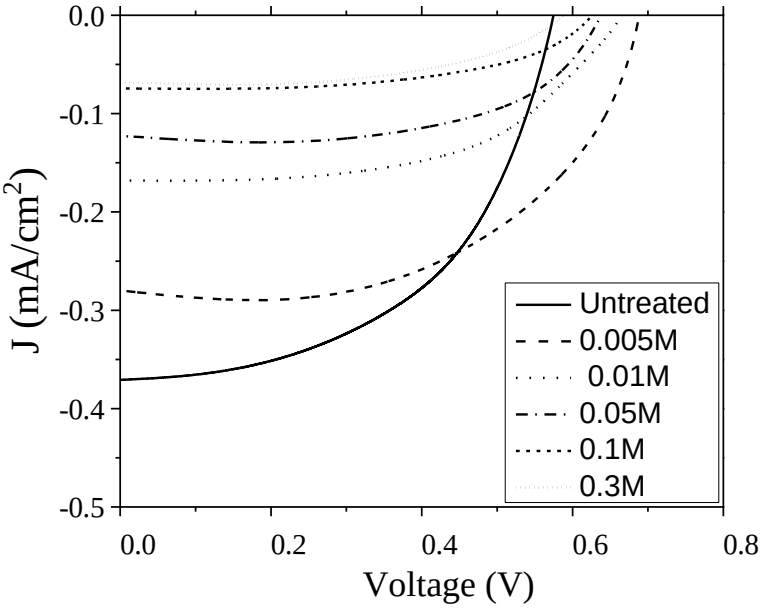

Figure 4.10. Current density versus voltage characteristic curves for the DSSCs sensitized with Trigonella foenum-graecum dye in the presence of ZnO layer on TiO_2 thin film.

Table 4.7. Photovoltaic parameters of the DSSCs sensitized by Trigonella foenum-graecum dye treated with ZnO layer on TiO_2 thin film.

Molarities	J_{sc} (mA/cm^2)	V_{oc} (V)	J_m (mA/cm^2)	V_m (V)	P_{max} (mW)	FF	η_{eff} %
Untreated	0.370	0.574	0.276	0.409	0.111	0.532	0.113
0.005M	0.284	0.690	0.222	0.489	0.109	0.554	0.109
0.01M	0.169	0.664	0.133	0.472	0.063	0.559	0.063
0.05M	0.121	0.637	0.100	0.477	0.048	0.619	0.048
0.1M	0.076	0.626	0.058	0.463	0.026	0.564	0.027
0.3M	0.068	0.592	0.051	0.422	0.023	0.535	0.022

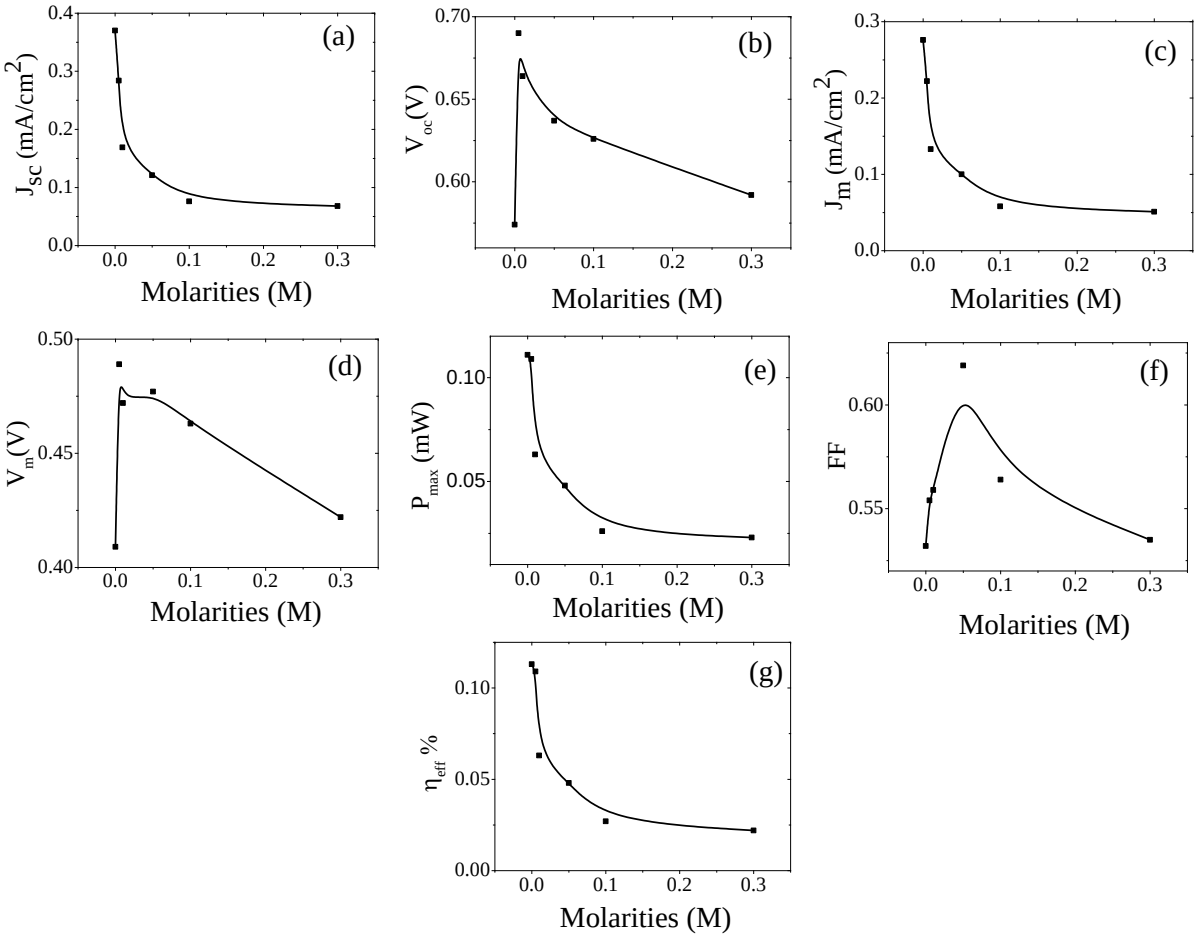

Figure 4.11. Represents the relation between molarities and different parameters (a : J_{sc}, b : V_{oc}, c : J_m, d : V_m, e : P_{max}, f : FF, and g : η_{eff}) for DSSCs sensitized by Trigonella foenum-graecum dye treated with ZnO layer on TiO_2 thin film.

4.8. Open-circuit voltage decay measurements

In solar cells the recombination process plays an important role in decreasing its performance since many research was performed to reduce this process. The transition of electrons from TiO_2 conduction band to oxidized electrolyte is considered as one kind of recombination processes in DSSCs [37]. The velocity of recombination can be detected by using electron lifetime which is defined as average lifetime it takes for an electron to be recombined. A long electron lifetime is considered as critical factor for high performance of solar cell. The relation between electron recombination lifetime and recombination process is reversal. The electron lifetime (τ_e) was determined by the reciprocal of the derivative of the decay curves normalized by the thermal voltage (k_BT/e), using Eq.4.1 then, curves representing the relationship between the resulting τ_e and V_{oc} were drawn [38]. In another way, electron recombination lifetime of DSSCs was determined by fitting the data obtained from V_{oc}-*Time* curve by using Eq.4.2 [39]. Figure 4.12 represent open circuit voltage curve that describe dark and light regions.

$$\tau_e = -\frac{k_BT}{e}\left(\frac{dV_{oc}}{dt}\right)^{-1} \tag{4.1}$$

Here, K_BT is the thermal energy, e is the positive elementary charge, and dV_{oc}/dt is the linear part of the voltage decay curve

$$V = V_0 - A_1 \exp[-(t - t_1)/\tau_e] \tag{4.2}$$

where τ_e is the electron lifetime, V_0 and A_1 are fit parameters, and (t-t_1) the time in dark region.

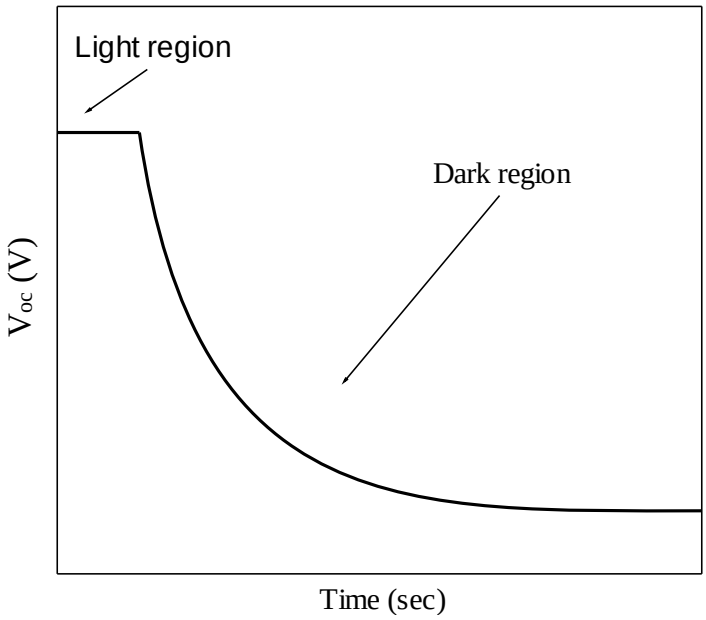

Figure 4.12 Open-circuit voltage decay curve.

This study was conducted for DSSCs sensitized with Trigonella foenum-graecum dye. The open-circuit voltage versus time curves for untreated and for the treated DSSCs with ZnO layer deposited by SILAR method at concentrations of 0.005M, 0.01M, 0.05M, 0.1M, and 0.3M of $ZnCl_2$ solutions are shown in Figure 4.14, and at different incident light intensities are shown in Figure 4.15. The relation between electron lifetime (τ_e) and open-circuit voltage for untreated DSSCs and treated ones at different concentrations are shown in Figure 4.16. τ_e versus V_{oc} at different incident light intensities for untreated and treated ones are shown in Figure 4.17. Table 4.8 represent electron recombination lifetime at different intensities of untreated and treated ones at different concentrations. Figure 4.15 shows that the largest V_{oc} value was at 1 sun intensity and when light intensity decrease, the value of V_{oc} decreased for all cells . Figure 4.15 and 4.17 represents the reversal relation between V_{oc} and electron recombination lifetime. From Table 4.8, the largest lifetime value for electron recombination of 12.25 s was for ZnO treatment of DSSC at 0.005M of $ZnCl_2$ solution, whereas the lowest value of 6.73 s was for untreated cell. When concentration of $ZnCl_2$ solution increased, the electron recombination lifetime decreased. The decay time of the voltage signals can indicate to the speed of the recombination process as the value of lifetime

increased, the electron recombination process reduced. Electron recombination process was the least at 0.005M but it was the largest for untreated cell and this indicated that ZnO acts as a barrier layer by blocking the electron injection from TiO_2 into the excited-state dye. The photo- injected electrons in the conduction band of TiO_2 can only recombine with the reductive agent by tunnelling through the ZnO at the interface. Figure 4.13 show energy level for DSSC component.

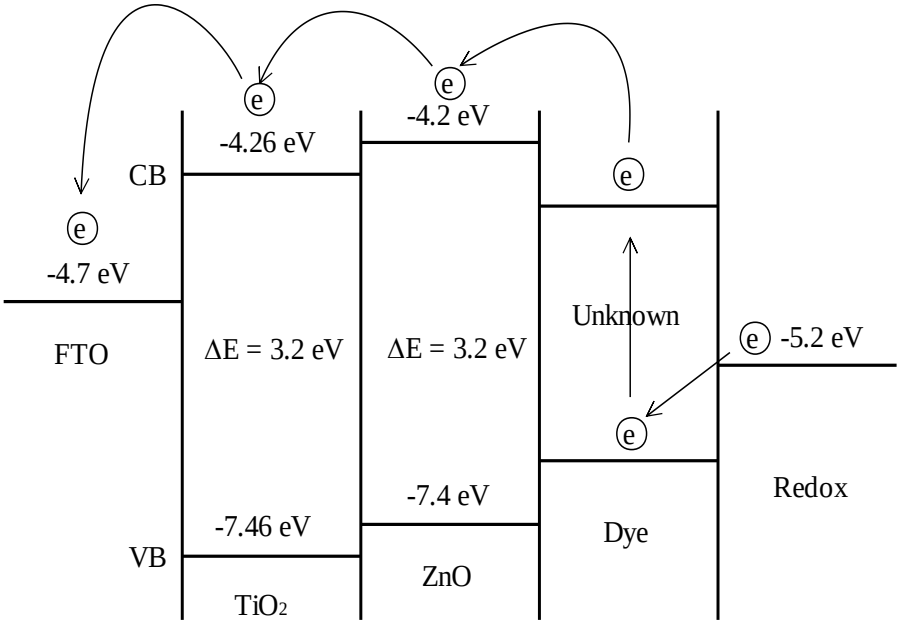

Figure 4.13 Energy levels of the DSSC components.

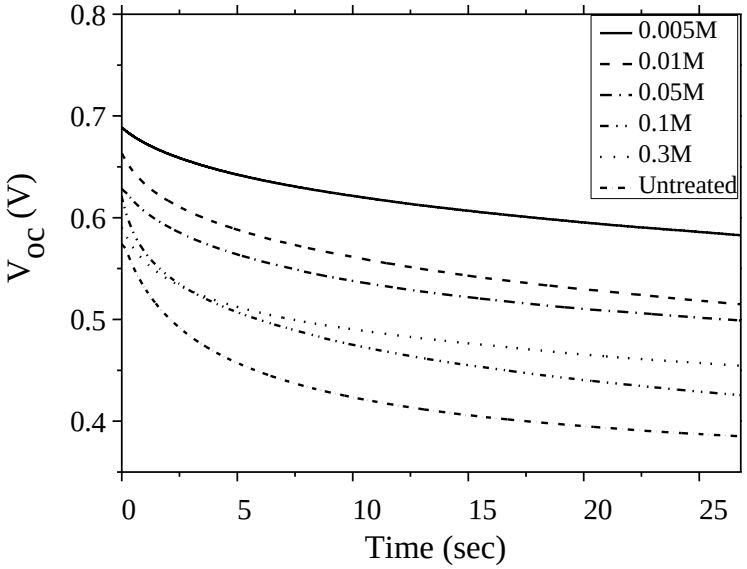

Figure 4.14. Open-circuit voltage decay for the untreated DSSCs and treated ones with ZnO layer at 0.005M, 0.01M, 0.05M, 0.1M, and 0.3M of $ZnCl_2$ solutions .

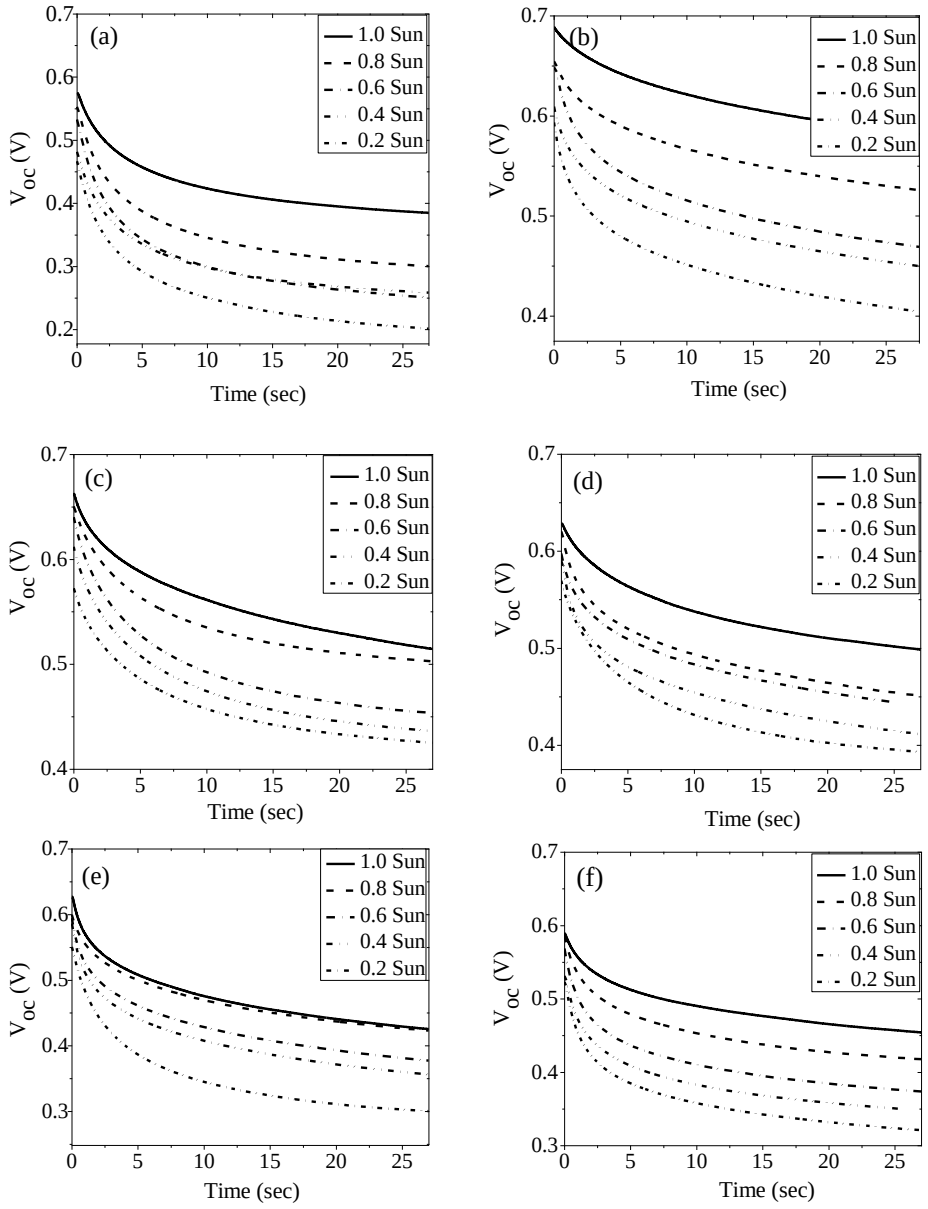

Figure 4.15. Open-circuit voltage decay for the DSSCs at different incident light intensities for untreated one (a), treated cells with ZnO layer at 0.005M (b), 0.01M (c), 0.05M (d), 0.1M (e), and 0.3M of $ZnCl_2$ solutions (f).

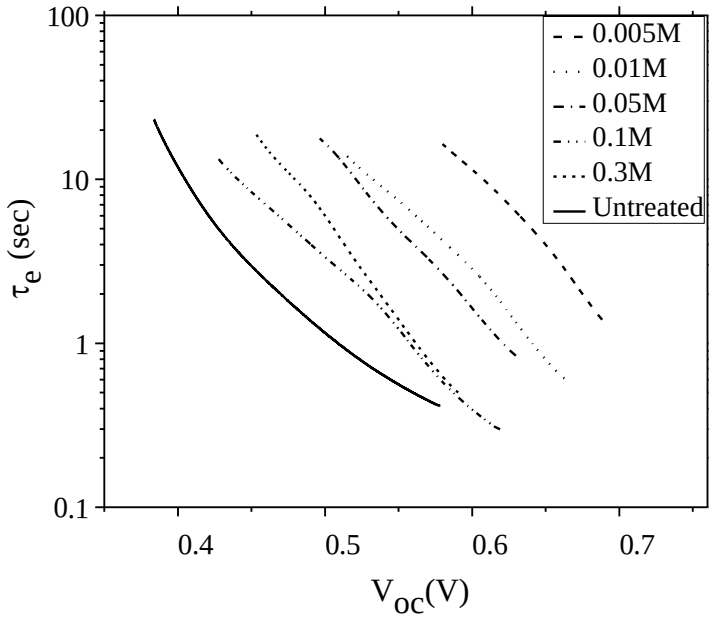

Figure 4.16. Electron lifetime versus open-circuit voltage for untreated DSSCs and treated ones with ZnO layer at 0.005M, 0.01M, 0.05M, 0.1M, and 0.3M of $ZnCl_2$ solutions .

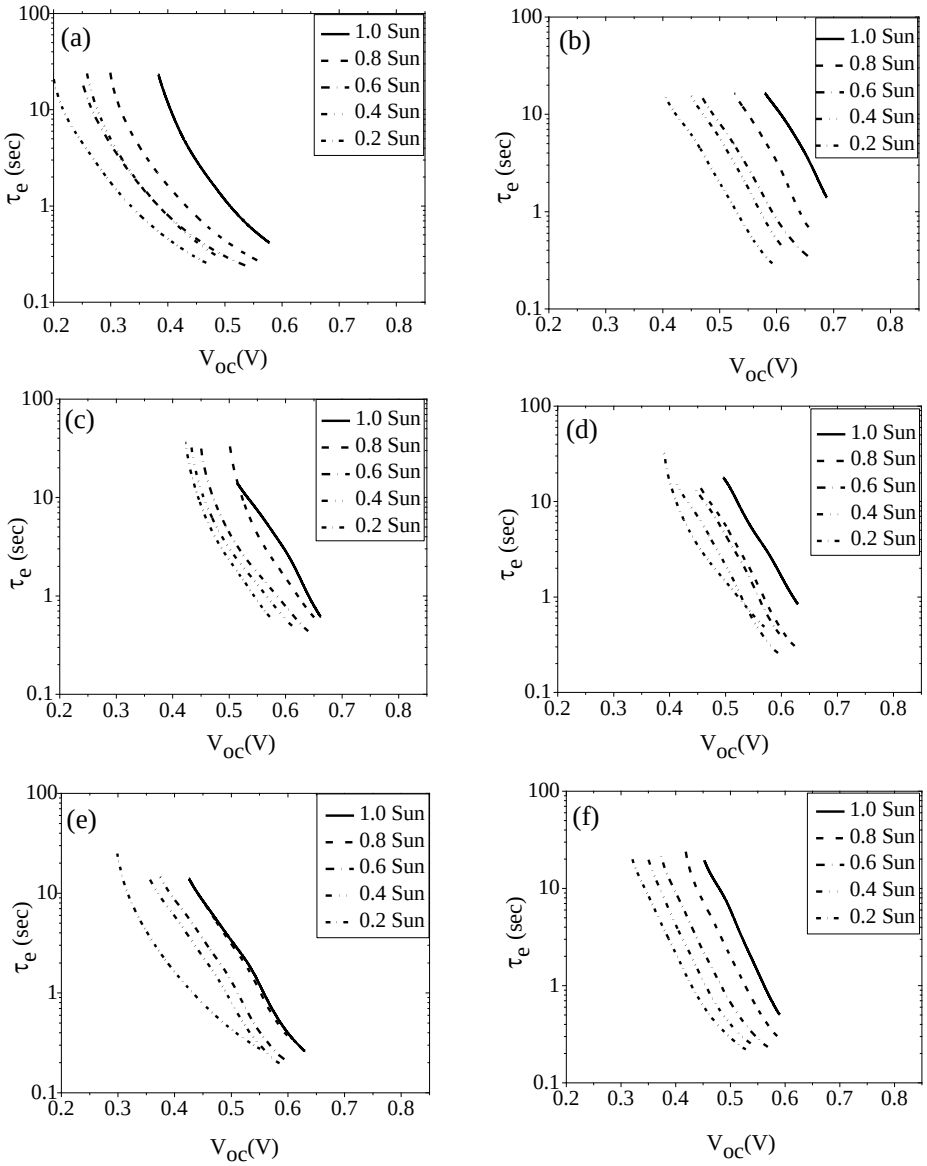

Figure 4.17. Electron lifetime versus open-circuit voltage at different incident light intensities for untreated one (a), treated with 0.005M (b), 0.01M (c), 0.05M (d), 0.1M (e), and 0.3M of $ZnCl_2$ solutions (f).

Table 4.8. Electron recombination lifetime of untreated and ZnO treated DSSCs.

Intensity (Sun)	Untreated	0.005M	0.01M	0.05M	0.1M	0.3M
	τ_e (sec)	τ_e (sec)	τ_e (sec)	τ_e (sec)	τ_e (sec)	τ_e (sec)
1.0	6.73	12.52	11.04	9.60	8.47	7.70
0.8	5.86	10.57	7.20	8.38	7.90	6.11
0.6	5.78	8.10	7.15	7.18	6.59	5.27
0.4	5.74	7.96	6.96	6.82	6.22	5.19
0.2	5.73	6.99	5.00	5.10	5.90	5.14

CONCLUSIONS

The main aim of this work was to investigate the performance of DSSCs sensitized with natural dyes extracted from plant seeds and to study the effect of several treatments on the performance of these cells such as pre-treatment of FTO glass substrates using several acids, post-treatment of TiO_2 layer, different pH of dye solution, ZnO thin film as a barrier layer, and open circuit voltage decay measurements. Ten natural dyes extracted from plant seeds have been tested as sensitizers for DSSCs. The DSSCs sensitized with Trigonella foenum-graecum, Apium graveolens, and Rhus were observed to have the best performance so they were chosen for further investigations. The DSSCs sensitized with Trigonella foenum-graecum showed the highest efficiency of 0.098%. The results showed decreasing in efficiency for FTO and TiO_2 of DSSCs sensitized with Trigonella foenum-graecum dye treated by different acids but FF increased for FTO treated with H_3PO_4 to 2% and with HNO_3 to 4.4% whereas improved to 2.9% for TiO_2 treated with HNO_3. The results related to DSSCs sensitized with Apium graveolens dye represented increasing FF for TiO_2 to 1.7% and 6% when using HNO_3 and HCl respectively and also the results showed improving in V_{oc} for FTO when treated with H_3PO_4 and HNO_3 to 3.9% and 5.1% respectively. The efficiency decreased for FTO and TiO_2 of DSSCs sensitized with Apium graveolens dye. The effect of changing the pH values of the dye solution using acetic and hydrochloric acids was decreasing the DSSCs efficiency. The addition of ZnO layer at 0.005M, 0.01M, 0.05M, 0.1M, and 0.3M of $ZnCl_2$ solutions on TiO_2 film showed an enhancement in open circuit voltage by 20.2%, 15.7%, 11%, 9%, and 3.1% and enhancement in fill factor by 4.1%, 5%, 16.35%, 6%, and 0.56% respectively while the efficiency reduced. 0.005M was the best concentration corresponding to highest open circuit voltage. It improved V_{oc} from 0.574 V to 0.690 V showing an enhancement of 20.2%. The open circuit voltage decay measurements were conducted for untreated DSSCs and those treated with ZnO barrier layer at different concentrations of $ZnCl_2$ solutions. The treated DSSCs

showed increasing in lifetime for highest value was 12.52 s at 0.005M and when concentration increased lifetime decreased. The lowest lifetime was 6.73 s for untreated cell and that indicate the recombination process was suppressed.

References

[1] K. P. Schröder and R. Connon Smith, " Exoplanets" **,** Praxis Publishing, UK, (2008).

[2] M. Grätzel, "Molecular photovoltaics mimic photosynthesis", Nature, Vol. 414, No.15 , pp. 338–344, (2001).

[3] M. A. Green, "Solar cells: operating principles, technology, and system applications", Prentice-Hall, USA, (1982).

[4] M. Zeman, "Introduction to photovoltaic solar energy", South Holland, Delft, (2012).

[5] M. H. Bohra, "Process development for single-crystal silicon solar cells", M.Sc. Thesis, Kate gleason college of engineering, New York, (2014).

[6] K. Shankar, G. K. Mor, H. E. Prakasam, O. K. Varghese, C. A. Grimes, " Self-assembled hybrid polymer-TiO_2 nanotube array heterojunction solar cells", The Journal of Physical Chemistry, Vol. 23, No. 24, pp. 12445-12449, (2007).

[7] S. Tepavcevic, S. B. Darling, N. M. Dimitrijevic, T. Rajh, S. J. Sibener, "Improved hybrid solar cells via in situ UV polymerization" , Small, Vol. 5, No. 15, pp. 1776-1783, (2009).

[8] J. Roncali, Conjugated poly (thiophenes) "synthesis, functionalization, and Applications", Chemical Reviews. Vol. 92, No. 4, pp. 711 – 738, (1992).

[9] S. Günes, H. Neugebauer, N.S. Sariciftci, "Conjugated polymer-based organic solar cells", Chemical Reviews, Vol. 107, No. 4, pp. 1324–38, (2007).

[10] S. Sun, N. Sariciftci, "Organic photovoltaics: mechanisms, materials, and Devices", Chemical Rubber Company Press, Florida, (2005).

[11] F. G. Gao, A. J. Bard, and L. D. Kispert, "Photocurrent generated on a carotenoid-sensitized TiO_2 nanocrystalline mesoporous electrode", Journal of Photochemistry and Photobiology, Vol. 130, No. 1, pp. 49-56, (2000).

[12] C. Julian Chen, "Physics of solar energy", John Wiley & Sons, New Jersey, (2011).

[13] C. Gueymard, "Parameterized transmittance model for direct beam and circumsolar spectral irradiance", Solar Energy, Vol. 71, No. 5, pp. 325-346, (2001).

[14] Md. I. Khan, "A Study on the optimization of dye-sensitized solar cells", M.Sc. Thesis, University of South Florida, Florida, (2013).

[15] K. Hara, T. Horiguchi, T. Kinoshita, K. Sayama, and H. Arakawa," Influence of electrolytes on the photovoltaic performance of organic dye-sensitized nanocrystalline TiO_2 Solar cells", Solar Energy Materials & Solar Cells, Vol. 70, No. 2, pp. 151-161, (2001).

[16] G. Boschloo and A. Hagfeldt, "Characteristics of the iodide/triiodide redox mediator in dye-sensitized solar cells" Accounts of Chemical Research, Vol. 42, No.11, pp. 1819-1826, (2009).

[17] B. Hardin, "Increased light harvesting in dye-sensitized solar cells Using Forster resonant energy transfer", PhD Thesis, Stanford University, San francisco, (2010).

[18] R. Corkish, M. A. Green, M. E. Watt, S. R. Wenham, "Applied photovoltaics", Earthscan, USA, (2007).

[19] Green, M. A., " Photovoltaic principles", Science, Vol.14, No. 1-2, pp.11-17, (2002).

[20] D. M. Chapin, C. S. Fuller, G. L. Pearson, " A New silicon p-n junction photocell for converting solar radiation into electrical power", Journal of Applied Physics, Vol.25, No.5, pp.676-677, (1954).

[21] H. Tsubomura, M. Matsumura, Y. Nomura, T. Amamiya, "Dye sensitized zinc oxide: aqueous electrolyte: platinum photocell", Nature, Vol.261, No.5559, pp.402-403, (1976).

[22] B. G. O'Regan, M. Grätzel, "A low-cost, high-efficiency solar cell based on dye-sensitized colloidal TiO_2 films", Nature, Vol.353, No.24, pp.737-740, (1991).

[23] H. Ghamri, "Dye-sensitized solar cells using ZnO as a semiconductor layer", M.Sc. Thesis, Islamic Uuniversity of Gaza, Gaza, (2012).

[24] K. Refi, "Dye-sensitized solar cells using TiO_2 as a semiconducting layer", M.Sc. Thesis, Islamic Uuniversity of Gaza, Gaza, (2013).

[25] I.Radwan, " Dye sensitized solar cells based on natural dyes extracted from plant roots", M.Sc. Thesis, Islamic Uuniversity of Gaza, Gaza, (2015).

[26] www.metrohm-autolab.com

[27] http://www.kobis.si/prodajni-program/molekulska-spektroskopija/Genesys

%2010S%20UV-VIS.pdf

[28] http://www.unitechbrasil.com/index.php?option=com_phocadownload&view

=category&download=102:spectrophotometercrossreference&id=18:thermofisher&Itemid=107

[29] K. Hara, T. Horiguchi, T. Kinoshita, K. Sayama, H. Sugihara and H. Arakawa, "Highly efficient photon-to-electron conversion with mercurochrome-

sensitized nanoporous oxide a semiconductor solar cells", Solar Energy Materials & Solar Cells, Vol. 64, No. 2, pp. 115-134, (2000).

[30] I. Jinchu, C.O. Sreekala, and K.S. Sreelatha, " Dye sensitized solar cell using natural dyes as chromophores – review", Materials Science Forum, Vol. 771, No.1 , pp. 39-51, (2014).

[31] R.S. Shelke, S.B. Thombre and S.R. Patrikar, "Status and perspectives of dyes used in dye sensitized solar cells", International Journal of Renewable Energy Resources, Vol. 3, No. 2, pp. 12-19, (2013).

[32] S. Al-Bat'hi, A. Iraj, I. Sopyan, "Natural photosensitizers for dye sensitized solar cells", International Journal of Renewable Energy Research, Vol. 3, No. 1, pp. 138-143, (2013).

[33] K.F. Moustafa, M. Rekaby, E.T. El Shenawy and N.M. Khattab, "Green dyes as photosensitizers for dye-sensitized solar cells", Journal of Applied Sciences Research, Vol. 8, No. 8, pp. 4393-4404, (2012).

[34] L. Emily, "Theoretical study of dye-sensitized solar cell (DSSC)", M.Sc. Thesis, The University of Hong Kong, Hong Kong, (2009).

[35] A. Tangri, " Trigonella Foenum-Graecum Mucilage: An Adsorbent for Removal of Sulphate Ions" International Journal of Advanced Research in Chemical Science, Vol. 1, No. 7, pp. 34-42, (2014).

[36] W. Peng, W. Li-Duo, L. Bin, Q. Yong, "Improved voltage and fill factor by using zinc oxide thin film as a barrier layer in dye-sensitized solar cells", Science, Vol. 22, No.10, pp. 2708-2710, (2005).

[37] F. Santiago, J. Cañadas, E. Palomares, J. Clifford, S. Haque, J. Durrant, G. Belmonte, J. Bisquert, " The origin of slow electron recombination processes in dye-sensitized solar cells with alumina barrier coatings", Journal of applied physics, Vol. 96, No. 11, pp. 6903-6907, (2004).

[38] A. Zaban, M. Greenshtein, J. Bisquert, "Determination of the electron lifetime in nanocrystalline dye solar cells by open-circuit voltage decay measurements", European Journal of Chemical Physics and Physical Chemistry, Vol. 4, No. 8, pp. 859-864, (2003).

[39] Z. Zhang, "Enhancing the open-circuit voltage of dye-sensitized solar cells: coadSorbents and alternative redox couples", PhD thesis, Tsinghua University, China, (2008).